MINOR ACTINIDE WASTE DISPOSAL IN DEEP GEOLOGICAL BOREHOLES

By

CALVIN GREGORY SIZER

SUBMITTED TO THE DEPARTMENT OF NUCLEAR SCIENCE
AND ENGINEERING
IN PARTIAL FULFILLMENT OF THE REQUIREMENTS FOR THE DEGREE OF

BACHELORS OF SCIENCE IN NUCLEAR SCIENCE AND ENGINEERING
AT THE
MASSACHUSETTS INSTITUTE OF TECHNOLOGY

May, 2006

(June 2006)

The author hereby grants to MIT permission to reproduce and to distribute publicly
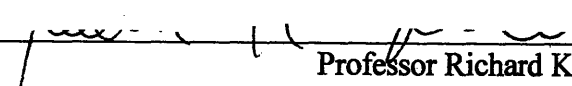Paper and electronic copies of this thesis document in whole or in part.

Signature of Author: _____
Calvin Gregory Sizer
Department of Nuclear Science and Engineering
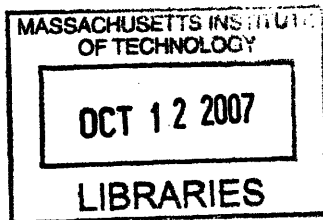May 2006

Certified by: _____
Michael J. Driscoll
Professor Emeritus of Nuclear Science and Engineering
Thesis Supervisor

Certified by: _____
Professor Richard K. Lester
Department of Nuclear Science and Engineering
Thesis Reader

Accepted by: _____
David G. Cory
Professor of Nuclear Science and Engineering
Chairman, NSE Committee for Undergraduate Students

MINOR ACTINIDE WASTE DISPOSAL IN DEEP GEOLOGICAL BOREHOLES

By

CALVIN GREGORY SIZER

Submitted to the Department of Nuclear Engineering on May 19th, 2006.

In Partial Fulfillment of the Requirements for the Degree of

Bachelor of Science in Nuclear Science and Engineering

ABSTRACT

The purpose of this investigation was to evaluate a waste canister design suitable for the disposal of vitrified minor actinide waste in deep geological boreholes using conventional oil/gas/geothermal drilling technology. The nature of minor actinide waste was considered, paying particular attention to nuclides whose decay energy and half lives were of relative significance to the minor actinide waste as a whole. Thermal Analysis was performed based on a reference borehole design, by Ian C. Hoag. The strategy of the thermal analysis is aimed at finding peak temperatures within the configuration, paying particular attention to the heat transfer under deep geological conditions in the air gap between the canister and the borehole. A first order economic analysis was made to compare the designed canister emplacement costs to that of intact spent fuel.

The results of this analysis show that three minor actinide nuclides dominate heat generation after ten years cooling: Cm-244, Am-241, and Am-243 account for 97.5% of minor actinide decay heat. These three nuclides plus Np-237 account for 99% of the minor actinide mass. The thermal analysis was based on an irretrievable canister design, consisting of a 5 meter long synroc waste form, with minor actinides loaded to 1% wt, an outer radius of 15.8 cm and inner annular radius of 8.5 cm. Filling the annulus with a vitrified technetium and iodine waste form was found to be feasible using a multi-stage emplacement process. This process would only be required for three of the fifty boreholes because technetium and iodine have low heat generations after 10 years cooling. The suggested borehole waste form has a maximum centerline temperature of 349C. The costs of drilling boreholes to meet the demand of 100,000MT of PWR waste are estimated to be 3.5% of the current nuclear waste fund, or about $9.6/kg of original spent fuel.

Thesis Supervisor: Michael J. Driscoll

Title: Professor Emeritus of Nuclear Science and Engineering

Acknowledgements

Professor Driscoll, your time, commitment, and interest in this project are an inspiration to me. Thank you most of all for your patient advice and constant help.

Special thanks to the NUPOC and Naval Reactors undergraduate matriculation programs for supporting a portion of my undergraduate career and providing meaningful and interesting work to start my professional career hereafter.

Ian Hoag, whose thesis is heavily reference in this document and who helped with many of the calculations. Your constant support and encouragement were what every undergraduate should have in his/her thesis writing process.

To my wife, whom I married in the process of writing this thesis. Your understanding and support throughout my undergraduate career were vital to my successful completion.

To my mother and father, who supported the vast majority of my undergraduate tuition and expenses. Thank you for your example and inspiration.

To my older sister, for her constant encouragement.

To Elkan Hawkins and David Legault. For their steady friendship.

To Jesus Christ, for inner peace and blessed assurance.

To the Faculty and Staff of the Nuclear Engineering Department, with special thanks to my advisor Professor Kadak, for readily available advice,

With Sincere Gratitude!

Table of Contents

5

List of Figures

List of Tables

1 Introduction

Nuclear power may be the most promising energy option for the world today. Emitting no greenhouse gases, and having an abundant energy supply potential, nuclear plants remain very competitive with other forms of energy production. The benefits of nuclear power have been overshadowed by the challenge of nuclear waste disposal since its inception. The United States is currently developing the Yucca Mountain Project, a mined nuclear storage facility. This facility is currently designed to store 70,000 metric tons of heavy metal (MTHM). The nuclear waste disposal needs of current reactors operating in the United States will exceed this storage capacity, not to mention the future waste needs of newly licensed reactors [1]. Similar challenges are posed in other countries. A small portion of the nuclear waste, the transuranic elements, have very long relative half lives, greater than one million years. This slow decaying waste gives rise to concerns about the durability of Yucca Mountain's man-made isolation barriers over the long-term (above 10,000 years) and have made deep geological boreholes attractive.

Deep geological boreholes can be drilled from three to five kilometers into the Earth's crust, and depending on the type of rock being drilled, can provide effective radionuclide retention over the long-term. Research has been performed confirming that water soluble molecules can be trapped in igneous rock formations such as granite for time periods on the order of millions of years [2]. With the advancement of drilling techniques for hot dry rock in geothermal applications, the feasibility and cost effectiveness of drilling boreholes that reach kilometers deep in igneous rock portions of the Earth's crust is increasing.

The deep geological borehole option has been given increased attention lately, particularly in England. A current study performed by researchers at the University of Sheffield concluded

8

that their design for deep geological disposal could "accommodate almost any type of HLW" [3]

There is currently considerable interest in reprocessing spent light water reactor fuel to remove minor actinides (transuranic elements except for uranium and plutonium) in the United States. The advanced fuel cycle initiative, formed in 2003 as an outgrowth of the Advanced Accelerator Applications (AAA) Program, has focused on separation as a means of considerably reducing major contributions to long-term high-level-waste radio-toxicity [4]. Recently, the GNEP (Global Nuclear Energy Partnership) has been proposed as a means to implement this strategy [5]. This method of waste disposal would, in principle, simplify the licensing of Yucca Mountain. By separating minor actinides from light water reactor nuclear waste, hazards to people and the biosphere are greatly reduced in the very long-term. Figure 1-1 shows the proposed UREX+ process streams. Currently, the approach involves subsequent destruction of minor actinides by fission and/or transmutation of minor actinides in fast or thermal reactors, in mixed-oxide or fertile-free fuel. The alternative proposed in this investigation is to convert the minor actinides into a highly insoluble waste form, synroc, and place them in deep boreholes. Deep boreholes provide the necessary assurance of effective sequestration.

UREX$^+$

Spent Fuel
↓
UREX ⟶ U (Recycle or LLW)
⟶ Tc ("Safe Disposal")
⟶ I ("Safe Disposal")
↓
CDC-PEG ⟶ Cs/Sr ("Decay Storage")
↓
NPEX ⟶ Np/Pu (Thermal Recycle)
↓
TRUEX ⟶ FPs (Repository)
↓
Cyanex 301 ⟶ Am/Cm (Fast Recycle)
↓
Rare Earths (Repository)
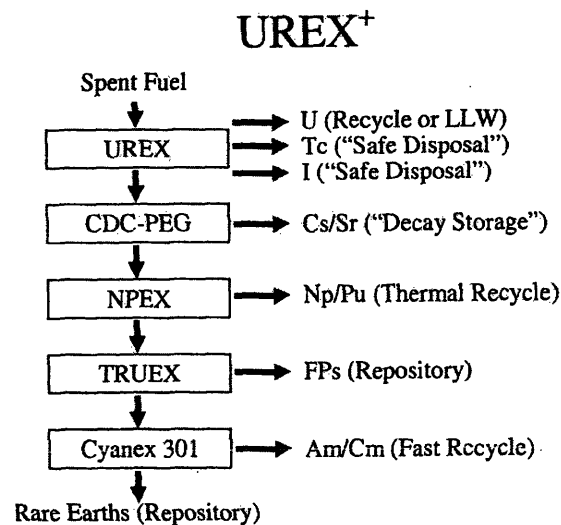
Figure 1-1 UREX+ Process [6]

1.1 Nuclear Waste

Radioactive waste generated from commercial reactors in the United States can be characterized in two categories, actinide and fission product waste. Fission products, as the name suggests, are created in a reactor by the bombardment of uranium atoms with neutrons. This interaction divides the uranium atom into a host of fragments, including more neutrons, each carrying a portion of the kinetic energy associated with the collision. Transuranic waste is created in the reactor by the capture of the incident neutron by the uranium atom, and subsequent radioactive decay which changes the elemental nature of the atom. The largest amount of commercial radioactive waste, by mass, is actinide waste, with the majority of the waste being U-238. Roughly six percent of the commercial waste is in the form of fission products. Although the percentage of fission product and minor actinide waste produced in commercial reactors is relatively small, this waste produces significant decay heat. Figure 1-2 shows the relative mass and thermal power components of an initial mass of one metric ton of uranium discharged from a commercial PWR after ten years cooling. This information was generated by the program ORIGEN, which is further explained in the next chapter. Table A-1 shows the numerical values from which Figure 1-2 was prepared.

10
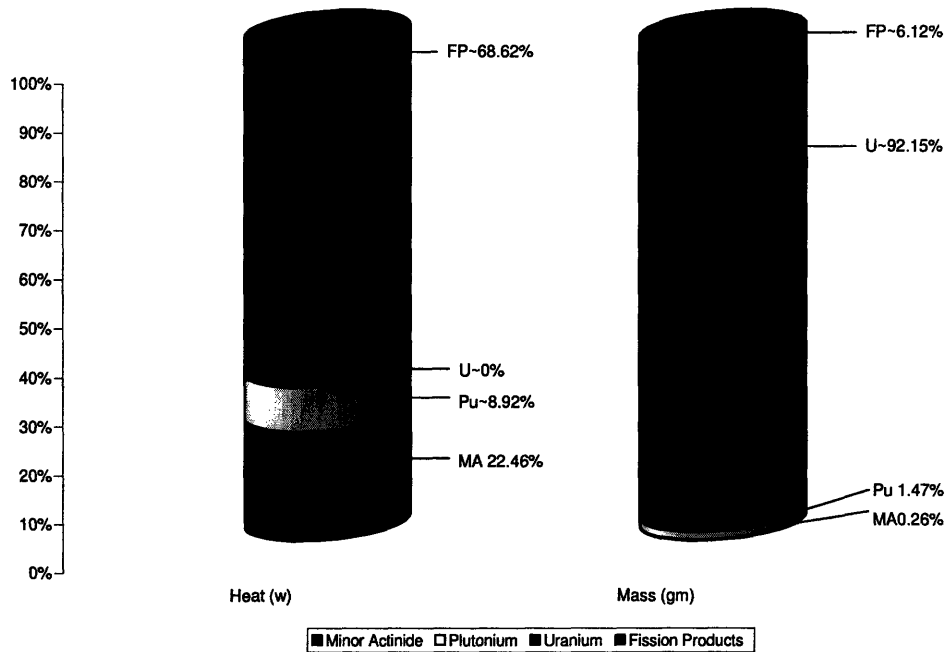
Figure 1-2 Commercial PWR Waste Breakdowns for 1 MTIHM, 60,000 MWD/MTHM Burnup, and 10 year cooling

Of the categories of waste shown in Figure 1-2, the minor actinides and plutonium pose the greatest economic, technical, and political challenge concerning the viability of Yucca Mountain, and most other shallow mined repositories. While the first sixty 60 yrs of thermal power dissipated by nuclear waste is dominated by fission products, the thermal power dissipation thereafter is dominated by the actinide elements. This phenomenon is because of the characteristic long half-lives of the actinide elements. The actinides with the largest contribution to thermal power in commercial nuclear waste are americium, plutonium, and curium. After nearly 200 yrs, the thermal power is almost entirely dominated by the actinide elements. Figure 1-3 displays the thermal power of nuclear waste over time as generated by ORIGEN. Given that 55% of the waste designated to be stored at Yucca Mountain is from PWR's, and the waste will have an average age in excess of 20 years cooling time, the minor actinides and plutonium will dominate the thermal power of the waste for nearly 97% of a 10,000 year period [7].

11
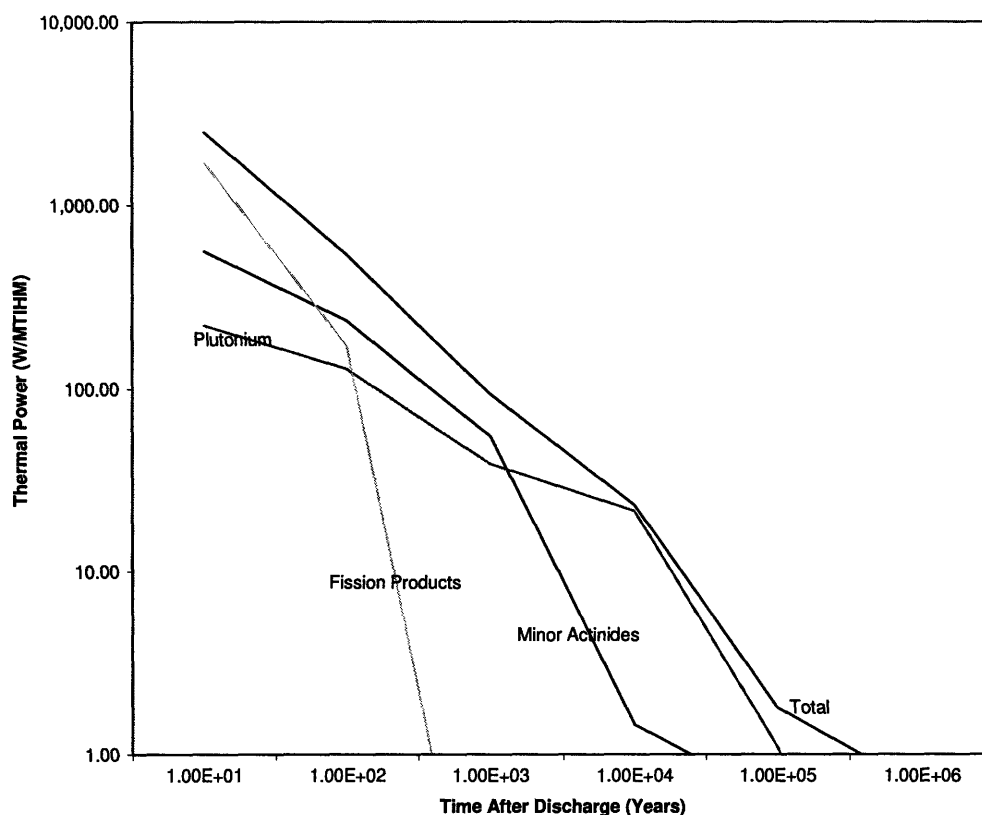
Figure 1-3 Commercial PWR Waste Thermal Power History for 1 MTIHM, 60,000 MWD/MTHM Burnup, and 10 year cooling

The long half lives of actinides in nuclear waste, as shown in Table 2.3, are constraining factors in long-term nuclear waste disposal. They are becoming more evident because recent regulatory limits have lengthened repository design standards for Yucca Mountain to extend to one million years [8]. One should note that it is not just thermal power, but radionuclide toxicity and escape transport properties which determine storage effectiveness. In fact, one study performed by researchers at Argonne National Laboratories indicates that the benefit of separating plutonium and americium alone will reduce the Yucca Mountain repository size by a factor of 4.3 to 5.4 for a given capacity [9].

1.2 Transmutation of Minor Actinides and Selected Fission Products

Current research investigating the separate disposal of long-lived radioactive waste is centered on the partitioning and transmutation method. Partitioning is the separation of long-

lived radioactive waste by chemical processes. Transmutation, much like nuclear fission, is the bombardment of long-lived radioactive waste with either neutrons from a reactor, or protons from a linear accelerator. The goal of transmutation is the fission of long-lived radioactive waste into shorter-lived radioactive fragments. Transuranics, as well as particularly radiotoxic, heat generating, or long-lived fission products are being considered for transmutation. In order to prevent the subsequent creation of more actinide waste by the capture of neutrons in uranium, a thorium oxide fertile fuel has been proposed for one method of transmutation. The advantage of thorium is that it has a fission capture cross section comparable to that of U-235, so it maintains a similar neutron economy. However, because thorium is lower on the periodic table than uranium, it limits the creation of plutonium and minor actinides. Thorium oxide also has a higher thermal conductivity that that of uranium oxide [10].

The disadvantage of using thorium to prevent the subsequent creation of plutonium and minor actinides is its chemical inertness, and the highly radioactive U-232 by-product [11]. Transmutation can also be a lengthy process. Transuranic waste must be separated and transmuted, then the process must be repeated until the waste has been efficiently annihilated. One study estimates a seven year period between when the waste is initially transmuted and when it can be placed back into a reactor for further transmutation [12]. Also, loses due to minor inefficiencies in the separation process, called reprocessing losses, lead to a relatively small amount (0.1% wt) of actinide waste that still requires permanent storage [13].

Another suggested method of transmuting nuclear waste is the use of inert matrix fuels [14]. This proposed method suggests transmutation by strategically inserting transmutable materials into current reactors for subsequent destruction.

1.3 The Borehole Concept

Interest in depositing nuclear waste in deep geological boreholes is increasing. A deep geological borehole is a hole drilled in a stable part of the Earth's crust, between three and five kilometers into which nuclear waste can be emplaced. The natural barriers of rock such as granite provide economic advantages over the costly and less reliable man-made barriers in mined repositories. Waste can be emplaced in the lowest one to two kilometers of the borehole and a backfill sealant in the upper portion. This concept is attractive because it provides high

isolation potential, reduced risk of diversion for weapon proliferation, a wide range of potential locations, and decreased surface temperature influence [15]. Thus, the analysis in this thesis is focused on modifications to a canister design developed for intact spent fuel disposal [Ian Hoag] that will allow for the emplacement of vitrified minor actinide waste and/or selected fission products in deep boreholes.

1.4 Reference Spent Fuel Canister

Figures 1-4 and 1-5 are display the single canister and borehole designs for the reference case spent fuel deep borehole designed by Ian C. Hoag. These figures will be helpful in visualizing the geometry of the borehole and will be referenced throughout this thesis.
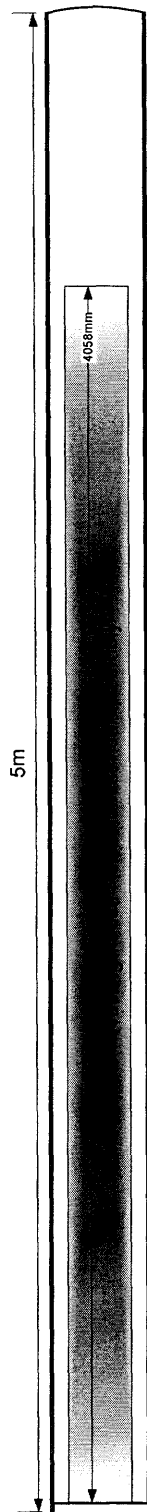
Figure 1-4 Individual Canister [16]
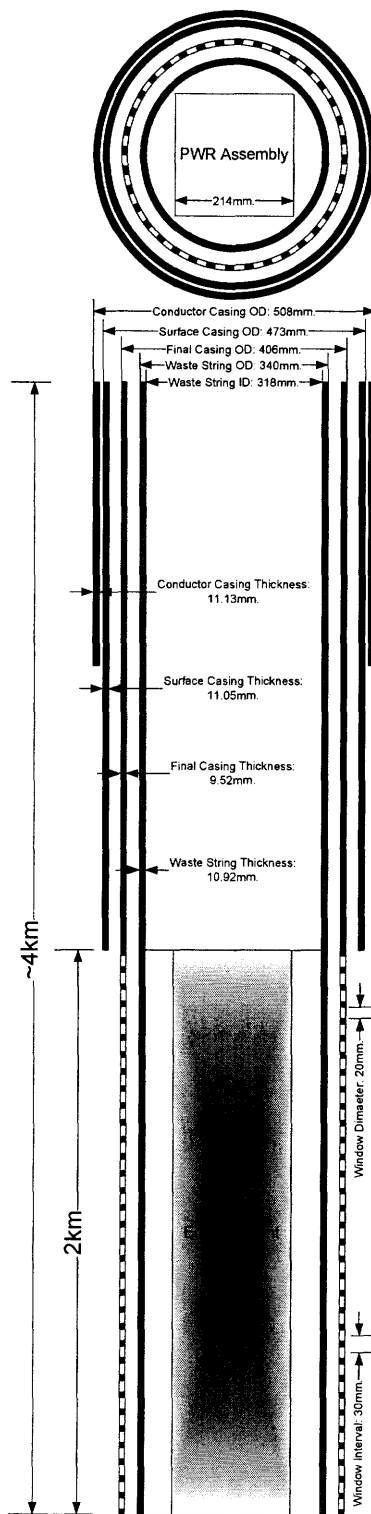
Figure 1-5 High Level Waste Borehole [17]

2 Energy Calculations

2.1 Reference Scenario Waste Assumptions

The mass and power of minor actinides shown in appendix A were calculated using ORIGEN. ORIGEN is a computer simulation of complex equations describing the concentration and activity of the different elements of nuclear fuel described in the introduction. It contains comprehensive decay, cross section, and photon data libraries for most actinides, fission products, and reactor materials [18]. Developed at Oak Ridge National Laboratories, this software is useful in displaying the mass, power, activity, and concentration as a function of various parameters.

The quantities generated in ORIGEN will be used as the reference case for further calculations in this analysis. The minor actinide mass and power were calculated under the assumption that the waste was generated by a pressurized water reactor with a 17X17 assembly arrangement. Further assumptions include: a 60,000 MWD/MTU burnup, a 4.2 percent uranium-235 fuel enrichment, a ten year cooling period, and each assembly experiencing three eighteen month cycles in a reactor which has a capacity factor of 85%.

2.2 Mass and Thermal Power at Ten Years

Table A-2 in appendix A lists the mass and thermal power for transuranic waste for the reference conditions listed in section 2.1. This analysis assumes that the uranium and plutonium nuclides will be separated from the mixture before immobilization and used for further energy production. Because the plutonium and uranium nuclides will be separated from the mixture they are noted as "excluded" in the comments section of appendix Table A-2. The nuclides labeled negligible in the comments section of Appendix A-2 are considered to be

17

negligible for future thermal analysis for one or more reasons. These nuclides have a mass that is less than one gram, or/and a thermal power of less than one watt after ten years cooling time. Also, many of these nuclides have relatively short half-lives.

The bolded nuclides in appendix Table A-2 are the substances of most significance because they have mass and thermal power quantities that account for most of the minor actinide waste mass and thermal power. To calculate the total energy and power produced by minor actinides the decay energy emitted by the three largest contributors to total decay heat will be modeled. Am-241, Am-243, and Cm-244 produce a total of 97.5% of the decay power of the minor actinides at ten years. These three nuclides along with Np-237, a negligible contributor to thermal power, account for 99% of the total minor actinide mass at ten years. An additional 40.5 percent of minor actinide mass is composed of minor actinides that produce negligible thermal power. Tables 2-1 and 2-2 are condensed versions of appendix Table A-2. Table 2-1 shows: the total power and mass for all actinide waste, including plutonium and uranium, exclusively minor actinide data totals, and a "negligible" total that sums the mass and thermal decay power of nuclides that are neither uranium, or plutonium, nor contribute significantly to the total thermal power or mass of minor actinide waste. It is important to note that for every one initial metric ton of uranium that is irradiated in a PWR, 2.32kg of minor actinide waste will remain ten years after discharge. Table 2-2 shows that 2.3kg of the minor actinide waste remaining will be one of four nuclides.

Table 2-1 Relevant Actinide Totals generated in ORIGEN for 60,000 MWD/MTHM Burnup, 10 year cooling, and Initial Mass of 1 MTIHM

Nuclide	Total Power after Ten Years (w/MTU)	Mass after Ten Years (g/MTU)
Total	8.50E+02	9.38E+05
Minor Actinide Total	**5.29E+02**	**2.32E+03**
Negligible Total	1.31E+01	2.08E+01

Table 2-2 Largest Minor Actinide Contributors to Mass and Thermal Power generated in ORIGEN for 60,000 MWD/MTHM Burnup, 10 year cooling, and Initial Mass of 1 MTIHM

Nuclide	Total Power after Ten Years (w/MTU)	Mass after Ten Years (g/MTU)
Total Np-237	1.84E-02	9.14E+02
Total Am-243	2.63E+00	4.08E+02
Total Am-241	9.47E+01	8.27E+02
Total Cm-244	4.18E+02	1.48E+02
Significant Total	5.16E+02	2.30E+03

2.3 Special Consideration for Am-241, and Pu-241

As seen from the Tables 2-1 and 2-2, Cm-244 and Am-241 are the two major producers of thermal power in minor actinide waste. However, Am-241's mass and power levels are of particular interest. The mass and thermal power of Am-241 increase for the first one hundred years after discharge, according to the calculations performed in ORIGEN. The increase of mass and thermal power of Am-241 can be attributed to the decay of Pu-241 after discharge. Because waste cooling time is variable, and in view of the relatively short half life of Pu-241 (14.4 years), it will be assumed to decay instantaneously. This provides a conservative estimate for Am-241 mass for future thermal analysis, because Pu-241 will be separated from minor actinide waste before the latter is prepared for immobilization.

Figure 2-1 displays the nuclear decay accounting for the increase in Am-241. Table 2-3 shows relevant characteristics for these two nuclides.

Pu-241

$$\beta^- \qquad T_{1/2} = 14.4 \text{ years}$$
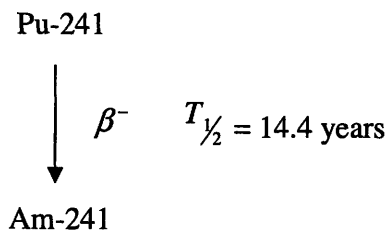
Am-241

Figure 2-1 Nuclear Decay Contributing to Rise in Am-241 Mass and Thermal Power

19

Table 2-3 Relevant Characteristics [19]

Nuclide	$T_{1/2}$ (y)	Energy (MeV)
Pu-241	14.4	0.021
Am-241	432.7	5.4857

Given the relatively short half life of Pu-241, 99% of the nuclide will have disintegrated into Am-241 in 100 years. Equation 2-1 is a differential relation between the atom densities of Am-241 and Pu-241. Equation 2-2 is the solution to Equation 2-1.

$$\frac{dN_{Am-241}}{dt} = \lambda_{Pu-241}N_{Pu-241} - \lambda_{Am-241}N_{Am-241}$$ 2-1

$$N_{Am-241} = \frac{\lambda_{Pu-241}N_{initialPu}}{\lambda_{Am-241} - \lambda_{Pu-241}} e^{-\lambda_{Pu-241}t} + Ce^{-\lambda_{Am-241}t}$$ 2-2

$$C = N_{initialAm-241} - \frac{\lambda_{Pu-241}N_{initialPu}}{\lambda_{Am-241} - \lambda_{Pu-241}}$$ 2-3

Calculations (Appendix B) were performed using the Am-241 and Pu-241 masses in appendix Table A-2, 827 and 1210 grams, respectively. These were used as initial conditions, where time zero starts ten years after discharge. The number density and mass of Am-241 as a function of time are:

$$N_{Am-241}(t) = -3.15\times10^{24}e^{-0.048t} + 5.22\times10^{24}e^{-0.002t} \, atoms$$ 2-3

$$Mass_{Am-241}(t) = [-1260.92e^{-0.048t} + 2089.53e^{-0.002t}] grams$$ 2-4

The number density and mass of Am-241 as a function of time represents the mass of Am-241 produced from one initial ton of uranium fuel in a PWR under the reference scenario conditions. Figure 2-1 was generated using MATLAB to plot the mass of Am-241 over one million years. The maximum mass of Am-241 is 1782.8 grams. Figure 2-2 shows Am-241 mass over time as calculated in ORIGEN. Note that the straight line segments are unphysical, and due only to the plotting program having only discrete data points as input. The maximum is confirmed (within ± 0.06 percent).
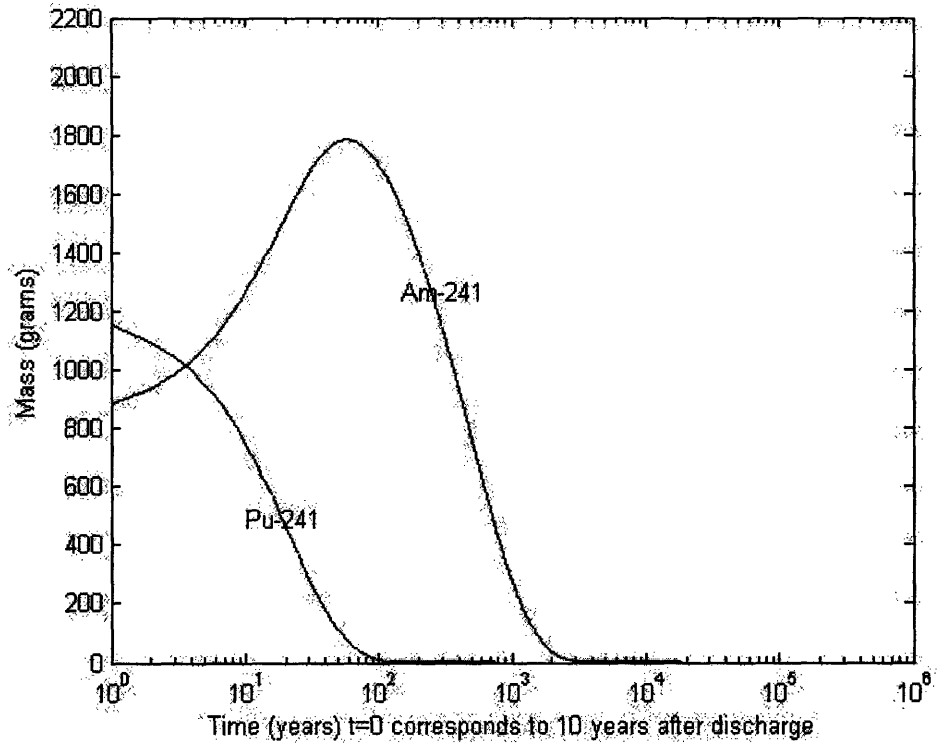
Figure 2-2 Mass of Am-241 and Pu-241 vs. Time using Pu-241 Decay Model for Reference Scenario
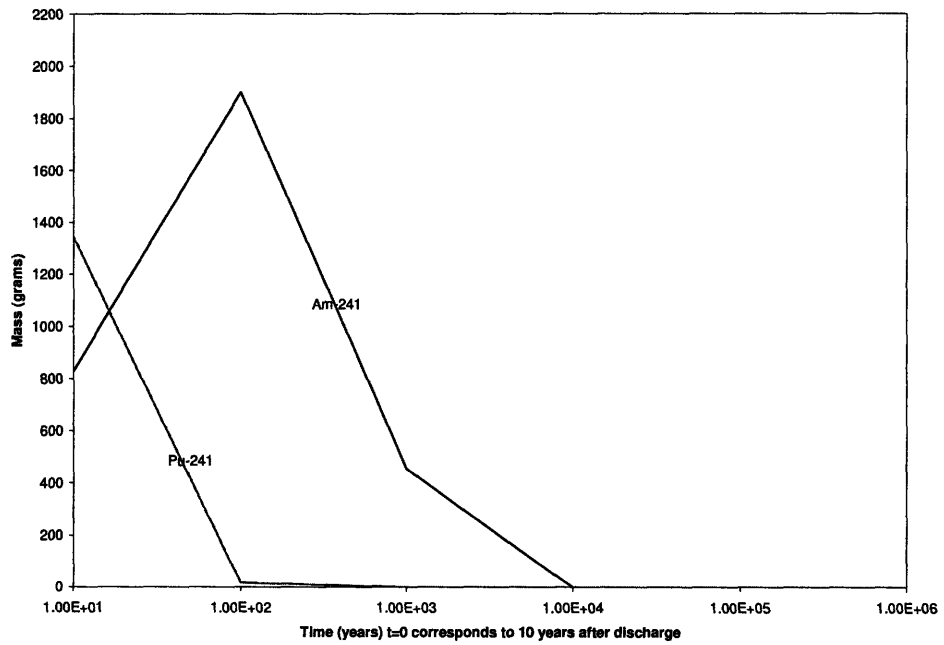
Figure 2-3 Mass of Am-241 and Pu-241 as calculated by ORIGEN for Reference Scenario

21

Table A-3 in the appendix shows all the mass values that are displayed in Figure 2-3. Corresponding values of thermal power are also included in this table.

2.4 Energy Calculations

2.4.1 Important Decay Chains

The total energy of minor actinide decay can be reasonably well modeled based on the total energy from three relatively energetic decays. The decay energy given off by the subsequent decay of daughter products has been included, however, daughter products with half-lives greater than one million years will be considered stable in the analysis.

Relevant Decay Chains:

Decay 1 $^{241}_{95}Am \longrightarrow {}^{237}_{93}Np + {}^{4}_{2}He$

Decay 2 $^{244}_{96}Cm \longrightarrow {}^{240}_{94}Pu + {}^{4}_{2}He$

$^{240}_{94}Pu \longrightarrow {}^{236}_{92}U + {}^{4}_{2}He$

Decay 3 $^{243}_{95}Am \longrightarrow {}^{239}_{93}Np + {}^{4}_{2}He$

$^{239}_{93}Np \longrightarrow {}^{239}_{94}Pu + \beta^{-}$

$^{239}_{94}Pu \longrightarrow {}^{235}_{92}U + {}^{4}_{2}He$
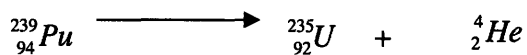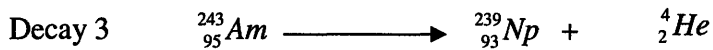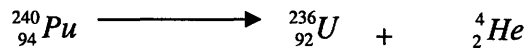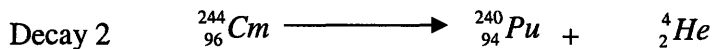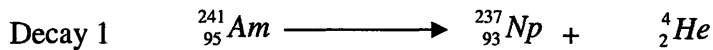
Table 2-4 will be useful for the next calculations and throughout this analysis. Relevant data on the important nuclides that dominate the power of minor actinide decay are shown.

Table 2-4 Table of Important Nuclide Characteristics [20]

Nuclide	$T_{1/2}$ (y)	Decay Energy (MeV)	Atomic Mass (amu)	Initial Mass (gm)
Am-241	432.2	5.638	241.0568229	827
Am-243	7370	5.438	243.0613727	408
Cm-244	18.1	5.902	244.0627463	148
Np-237	2.14 E06	--	237.0481673	--
Np-239	6.46 E-03	0.722	239.0529314	--
Pu-239	24110	5.245	239.0521565	--
Pu-240	6564	5.256	240.0538075	--
Pu-241	14.35	0.021	241.0568453	1210
U-235	7.04 E08	--	235.0439231	--
U-236	2.34 E07	--	236.0455619	--

2.4.2 Number Density of Pu-239 and Pu-240 versus Time

In order to calculate the total power of minor actinide decay, the number density of Pu-239 and Pu-240, must be calculated. Pu-239 and Pu-240 are the decay products of the nuclides that dominate thermal decay power. These number densities can be calculated using the model in equations 2-1 and 2-2. Because of its short half-life, Np-239 is assumed to decay instantaneously in these calculations. This analysis also assumes that the initial mass of Pu-239 and Pu-240 in spent fuel is separated and that the only mass presently decaying in a waste form will be that which arises from the decay of Cm-244.

$$N_{Pu-240}(t) = 3.662 \times 10^{23} (-e^{-0.038t} + e^{-1.056 \times 10^{-4} t}) atoms$$

$$N_{Pu-239}(t) = 1.456 \times 10^{24} (-e^{-9.405 \times 10^{-5} t} + e^{-2.875 \times 10^{-5} t}) atoms$$

2-5

2.4.3 Total Energy of Minor Actinide Decay

Per gram of nuclide having atomic mass A, and decay energy E_{decay}, the total energy emitted for complete decay is:

$$E_T = (\frac{E_{decay}}{A}) \times 9.65 \times 10^{10} \, Joules\,/\,gram \qquad\qquad \textbf{2-6}$$

The conversion factor is calculated by the conversion of units.

$$\frac{MeV}{amu} \times \frac{amu}{1.66 \times 10^{-27} kg} \times \frac{1kg}{1000 grams} \times \frac{10^6 eV}{1MeV} \times \frac{1.602 \times 10^{-19} Joules}{1eV} = 9.65 \times 10^{10} \, Joules\,/\,gram$$

Thus, Table 2-5 shows the total energy emitted for the nuclides in the three decay chains. Np-239 is absent from this list because of its short half life. Its decay energy was added to that of Am-243.

Table 2-5 Total Decay Energy of Relevant Nuclides

Nuclide	Total Decay Energy (J/gm)
Am-241	2.26E+09
Am-243	2.45E+09
Cm-244	2.33E+09
Np-239	2.91E+08
Pu-239	2.12E+09
Pu-240	2.11E+09
Pu-241	8.41E+06

2.5 Model for Power versus Time

From the total energy calculated in Table 2-5, the power can be calculated as:

$$P = E_T \times (\lambda N) \qquad\qquad \textbf{2-7}$$

Decay 1:

$$P_{Pu-241}(t) = 15.489 e^{-0.048t}$$

$$P_{Am-241}(t) = -180.45 e^{-0.048t} + 299.03 e^{-0.002t} watts$$

24

Decay 2:

$$P_{Cm-244}(t) = 403.07e^{-0.038t} watts$$

$$P_{Pu-240}(t) = 1.0314(-e^{-0.038t} + e^{-1.056 \times 10^{-4}t}) watts$$

Decay 3:

$$P_{Am-243}(t) = 2.9816e^{-9.405 \times 10^{-5}t} watts$$

$$P_{Pu-240}(t) = 0.1533(-e^{-9.405 \times 10^{-5}t} + e^{-2.875 \times 10^{-5}t}) watts$$

Figure 2-4 shows the power versus time curves of decay chain one, two, and three. All calculations are based on one metric ton of original heavy metal. The total power in Figure 2-4 is consistent with ORIGEN after the first ten years. The decay power from the model is 532 watts after ten years cooling, compared to 528 watts generated in ORIGEN. It should be noted that 13 of the 528 watts of power generated by minor actinides in the ORIGEN run are generated from nuclides not included in our model.
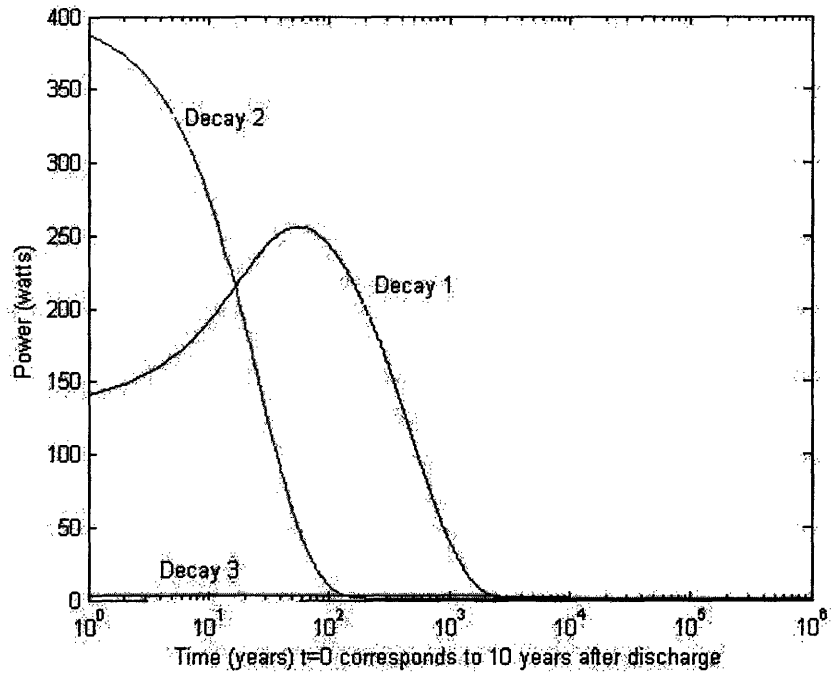
Figure 2-4 Calculated Decay Power vs. Time of Relevant Decay Chains for Reference Scenario
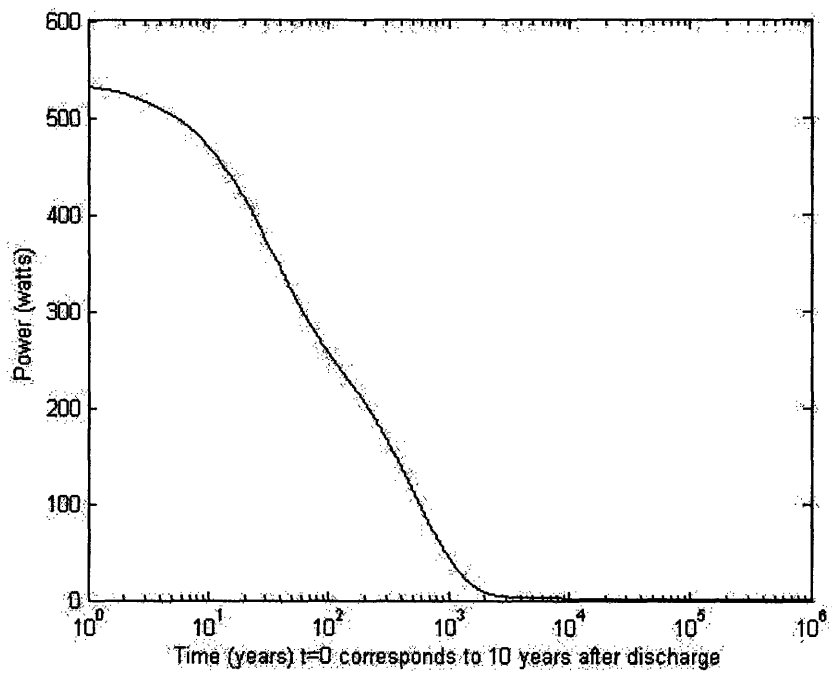
Figure 2-5 Calculated Total Decay Power vs. Time for Minor Actinide Waste Generated in Reference Case Scenario

ORIGEN confirms the basic trend of these calculations, as seen in Figure 2-6, below. Again, the segments between these points are artificially linearized.
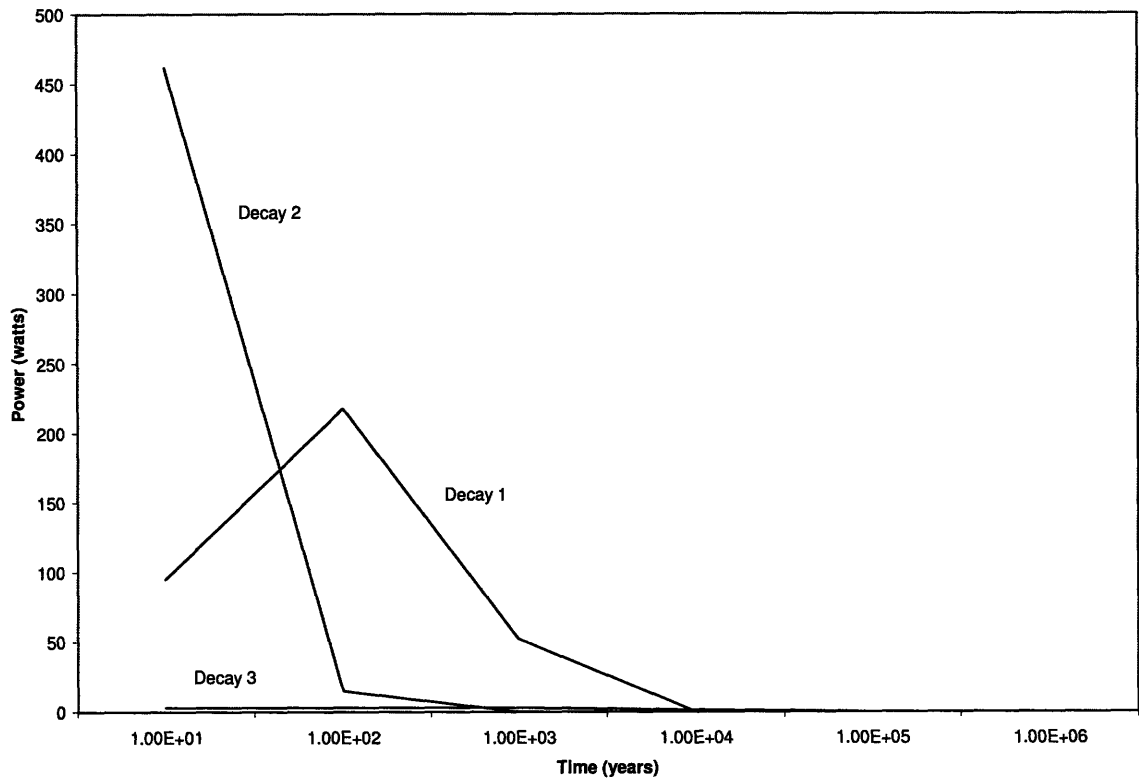
Figure 2-6 ORIGEN values for Cm-244, Am-241, and Am-243 Power vs. Time for Reference Scenario

2.5.1 Reference Linear Heat Rate

The linear heat rate, watts/m, will depend on the type of immobilization structure into which the minor actinides are vitrified. The design of the minor actinide waste canister may be limited by the chemical and structural capabilities of the canister and waste form, and the maximum temperature rise of the waste form or host rock. A discussion of the choice of immobilization form will be presented in Chapter 4. However, a maximum linear heat rate will be calculated presently for both types of immobilization forms in question. Table 2-6 shows the density and maximum weight percent loading for borosilicate glass and synroc.

Table 2-6 Properties of Immobilization Forms [21,22]

Parameter	Borosilicate glass	Synroc-C
Density (g/cm^3)	2.6	4.35
% of HLW	28%	30%

The volume of the reference canister (also known as the waste string), described in chapter 4, is needed. The dimensions of the canister are 15.77cm in radius and the length is 5m. These calculations assume that the glass or synroc will be molded to fit the inner dimensions of the canister. Space allowed for thermal expansion of the waste is considered negligible. The reference power is taken at ten years, which, by the model shown above is 532 watts per initial metric ton of uranium fuel. Also from Table 2-1, the total minor actinide mass ten years after discharge from one initial ton of uranium fuel is 2.32kg. The mass of each material in one canister is:

$$M_{glass} = 1016kg$$
$$M_{synroc} = 1699kg$$

Given the respective weight percents of glass and synroc, the mass of minor actinides per canister are:

$$M_{MAglass} = 284.5kg$$
$$M_{MAsynroc} = 509.7kg$$

The reference maximum linear heat rate can now be calculated:

$$q_{glass}' = 13250 \, ^W\!/_m$$

$$q_{synroc}' = 22200 \, ^W\!/_m$$

As will be shown, these values greatly exceed the limits set by the allowable thermal loading for the canister. Hence, the material loading in each immobilization form must be

reduced. The thermal analysis in chapter three will provide insight into how much the material loading must be decreased.

2.6 Summary

A couple of main conclusions can be drawn from analyzing the energy and mass histories of minor actinide waste. Ten years after discharge, minor actinide waste has trace elements of more than one hundred nuclides. However, most of the decay power and mass can be characterized by three or four nuclides. The thermal power was calculated for a period of one million years by relating the decay energy associated with three nuclide chains with their decay constants. The model was confirmed by results in ORIGEN. This model was ultimately used to find a reference maximum linear heat rate for subsequent thermal analysis.

3 Thermal Analysis

3.1 Methodology and Assumptions

The thermal analysis in this section is constructed around finding a maximum centerline temperature. This temperature will constrain the physical parameters of the waste-form. An empirical formula was used to estimate the peak temperature at the inner surface of a granite borehole as a function of linear heat rate. The centerline temperature was then calculated by using the peak granite wall temperature and evaluating the thermal resistances between the granite and the centerline. The effective thermal conductivity in the canister/borehole gap was calculated using an iterative process similar to that in Hoag's thesis [23]. This analysis has been simultaneously performed for both synroc and borosilicate glass. The equations in this chapter are relevant to both, but are shown for synroc for the purpose of continuity.

One major assumption made, in conjunction with Hoag's thesis, was the estimated value of the Earth's temperature gradient. The Earth's temperature gradient can vary depending on location and because of this the temperature at the depth of deep boreholes can vary greatly. A conservative 40 Celsius/km was assumed. For an emplacement zone of 2km, corresponding to a total depth of 4km, the Earth's pre-emplacement temperature was estimated to be as high as 160 degrees Celsius (433.15K).

3.2 Tables of Basic Data

Tables 3-1, 3-2, and 3-3 include relevant data for the thermal analysis that will follow in this chapter.

Table 3-1 Relevant Canister/Borehole Dimensions

Outer Diameter	$OD_{ws} := 339.7mm$	Outer Radius	$r_{od} = 16.985cm$
Inner Diameter	$ID_{ws} := 315.32mm$	Inner Radius	$r_{id} = 15.766cm$
Canister-Borehole Gap	$\delta_{gap2} = 1\ cm$	Canister Length	$L_{canister} := 5m$
Emplacement Length	$L_{emp} := 2km$		

Table 3-2 Relevant Material Properties

Thermal Expansion Coefficient of Synroc	$\beta_{synroc} := 10.5 \cdot 10^{-6} \cdot K^{-1}$	Thermal Conductivity of Synroc	$k_{synroc} := 2.1 \dfrac{W}{m \cdot K}$
Thermal Conductivity of Steel	$k_{steel} := 50.2 \dfrac{W}{m \cdot K}$	Thermal Conductivity of Granite	$k_{granite} := 2.4 \cdot \dfrac{W}{m \cdot K}$
Thermal Conductivity of Air	$k_{air} := 0.036 \dfrac{W}{m \cdot K}$	Waste/Canister Gap Heat Transfer Coefficient	$h_g := 31000 \dfrac{W}{m^2 \cdot K}$
Emissivity of Steel	$\varepsilon_1 := 0.8$	Emissivity of Granite	$\varepsilon_2 := 0.45$
Density of Synroc	$\rho_{synroc} := 4.35 \dfrac{gm}{cm^3}$		

Table 3-3 Other Constants

Semi-empirical Correlation Factor for Eq. 3-3	$B := 7$	Atmospheric Pressure	$P := 1atm$
Universal Gas Constant	$R_g := 8.3144 \dfrac{J}{mol \cdot K}$	Molecular Weight: Air	$m_{air} := 28.8 \dfrac{gm}{mol}$

3.3 Heat Transfer

3.3.1 Maximum Linear Heat Transfer Rate

The linear heat transfer rate is a variable of the design of the waste-form, including material and geometric properties. The previous chapter revealed that a synroc canister loaded with minor actinide wastes with no internal annular radius yielded a linear heat transfer rate of 22,200 W/m. Two properties: weight percent of minor actinides and annular radius, are variables in this analysis. A decrease in the weight percent of minor actinides in the waste-form will decrease its linear heat rate. Similarly, an increase in annular radius will decrease the linear heat rate. The mass of minor actinide waste in one canister is calculated in Equation 3-1. This equation yields mass as a function of weight loading and annular radius, where R_{id} is the outer radius, and R_1 is the annular radius.

$$M_2(wt, R_1) := wt \cdot \left(\rho_{synroc} \cdot \pi \cdot L_{canister} \right) \cdot \left| r_{id}^2 - R_1^2 \right|$$

3-1

Equation 3-2 is the effective maximum linear heat transfer rate as a function of weight loading and annular radius. Notice that 532 watts is the thermal power generated from the reference case of one initial metric ton of uranium, having a burnup of 60,000 MWD/MT, after ten years of cooling, and that 2.32kg is the mass of minor actinide waste generated in the reference case.

$$q'_{eff}(R_1, wt) := 532W \cdot \frac{1}{2.32kg} \cdot \frac{M_2(wt, R_1)}{L_{canister}}$$

3-2

3.3.2 Centerline Temperature

There are three significant temperature points which are calculated: the maximum temperature of granite, the maximum temperature of the canister's outer wall, and the maximum centerline temperature. To calculate the peak temperature of granite in a deep borehole setting, an empirical formula was used which determines peak granite temperature given linear heat rate [24]. Equation 3-3 shows the empirical formula as a function of the linear heat rate, the ambient temperature, thermal conductivity of granite, and the correction

factor B. The ambient temperature is taken to be the earth's temperature at the deepest point (4km) in the emplacement zone, 160C.

$$T_{granite} := T_{ambient} + \frac{q'_{eff}(R_1, wt)}{4 \cdot \pi \cdot k_{granite}} \cdot B$$

3-3

The temperature of the canister's outer wall was calculated using Equation 3-4. The effective thermal conductivity is the combined contributions of conduction, convection, and radiation. The effective thermal conductivity is discussed in more detail in Sections 3.4.2.1 and 3.4.2.3. The natural logarithmic function in Equation 3-4 accounts for the geometry of the cylindrical canister, and T_2 is the temperature on the outside surface of the canister.

$$T_2 := T_{granite} + q'_{eff}(R_1, wt) \cdot \frac{\ln\left[\frac{OD_{ws} + 2 \cdot \delta_{gap2}}{OD_{ws}}\right]}{2\pi \cdot k_{eff}}$$

3-4

The centerline temperature of the minor actinide waste form is calculated using Equation 3-5. This equation has three main components, starting with the temperature of the outside canister surface. The second component is the temperature increase due to the heat being generated in the waste form [25]. This component was modeled after a fuel pellet because it is a cylindrical heat generating solid, encapsulated by metal, similar to that of a fuel pellet. The third component of the equation arises from an annular design of the waste form. Discussion of the annular design will ensue in the next chapter.

$$T_{CLmax2} := T_2 + q'_{eff}(R_1, wt) \cdot \left[\frac{1}{4 \cdot \pi k_{synroc}} + \frac{1}{2 \cdot \pi \cdot r_o \cdot h_g} + \frac{1}{2 \cdot \pi \cdot k_{steel}} \cdot \ln\left[\frac{r_{od}}{r_{id}}\right]\right] - \frac{q'_{eff}(R_1, wt)}{4 \cdot \pi k_{synroc}} \cdot \left[1 - \frac{r_{id}^2}{r_{id}^2 - R_1^2} \cdot \ln\left[\frac{r_{id}^2}{R_1^2}\right]\right]$$

3-5

3.3.2.1 Conduction and Convection

The effective thermal conductivity used in the previous equations was calculated by the addition of the thermal conductivity due to convection and conduction, and the thermal conductivity due to radiation, shown in Equation 3-6.

33

$$k_{eff} := k_{rad1} + k_{eq1} \qquad \text{3-6}$$

The equivalent thermal conductivity for conduction and convection was calculated using the Prandtl, Grashof, and Rayleigh numbers shown in Equations 3-7, 3-8, and 3-9 respectively.

$$Pr := \frac{C_p \cdot v \cdot \rho}{k_{air}} \qquad \text{3-7}$$

$$Gr := \frac{g \cdot \left(T_2 - T_{granite}\right) \cdot \delta_{gap2}^{3}}{T_{avg} \cdot v^2} \qquad \text{3-8}$$

$$Ra := Gr \cdot Pr \qquad \text{3-9}$$

The specific heat and dynamic viscosity were all calculated using correlations from Hoag's thesis [11], shown in Equations 3-10 and 3-11. The kinematic viscosity is shown in Equation 3-12.

$$C_p := \left[0.0005 \cdot \left[\frac{T_{avg}}{K} - 273 \right]^2 + -0.3 \cdot \left[\frac{T_{avg}}{K} - 273 \right] + 1010 \right] \frac{J}{kg \cdot K} \qquad \text{3-10}$$

$$\mu := \frac{1.464 \times 10^{-6} \cdot \left[\frac{T_{avg}}{K} \right]^{1.5}}{\frac{T_{avg}}{K} + 113.299} \cdot Pa \cdot s \qquad \text{3-11}$$

$$v := \frac{\mu}{\rho} \qquad \text{3-12}$$

The correlation for conduction and convection within the gap is found in Fundamentals of Heat Transfer, shown in Equation 3-13 [26]. The effective heat transfer coefficient is shown in Equation 3-14, accounting for the annular shape of the canister.

$$k_{eq1} := k_{air} \cdot 0.18 \cdot Ra^{0.25}$$

3-13

$$h_{eq1} := \frac{k_{eq1}}{\dfrac{OD_{ws}}{2} \cdot \ln\left[\dfrac{OD_{ws} + 2 \cdot \delta_{gap2}}{OD_{ws}}\right]}$$

3-14

3.3.2.2 Radiation

The heat transfer coefficient and the effective thermal conductivity due to radiation were calculated using correlations from Hoag's thesis [27], shown in Equations 3-15 and 3-16.

$$h_{rad1} := \frac{\sigma}{\dfrac{1}{\varepsilon_1} + \left[\dfrac{OD_{ws}}{OD_{ws} + 2 \cdot \delta_{gap2}}\right] \cdot \left[\dfrac{1}{\varepsilon_2} - 1\right]} \cdot \left[\dfrac{T_2^4 - T_{granite}^4}{T_2 - T_{granite}}\right]$$

3-15

$$k_{rad1} := h_{rad1} \cdot \frac{OD_{ws}}{2} \cdot \ln\left[\frac{OD_{ws} + 2 \cdot \delta_{gap2}}{OD_{ws}}\right]$$

3-16

3.4 Summary

The thermal analysis used to find the temperature of the canister surface and the centerline temperature is dependent on the effective thermal conductivity of the canister/borehole gap. An iterative process and appropriate correlations were used to find the effective thermal conductivity. The solid waste-form was modeled after a fuel pellet. An appropriate modification to the fuel pellet temperature difference equation was made to account for an annular shape. Relevant geometric and material data were researched and integrated with the thermal power data from chapter two to produce an equation for the centerline temperature as a function of weight loading, and inner annular radius.

4 Canister Design

4.1 Introduction

As mentioned in the introduction, this thesis was written concurrently with Ian C. Hoag's master's thesis. As such, the design of the canister and recommendations for a purely minor actinide deep geological waste disposal are modifications to Hoag's spent fuel canister design. It may be assumed that any aspect of deep borehole design not specified in this section is the same as that in Hoag's thesis. The primary modifications to Hoag's reference design included in this section consist of nuclear waste form and retrievability.

4.2 Irretrievability

Unlike spent uranium and plutonium wastes, minor actinide waste will not be of potential use to satisfy future energy needs. The separation and fabrication processes required to obtain commercially viable products from minor actinide wastes such as Am-243 are uneconomical. Consequently, this waste is of no use and retrievability mechanisms included in Hoag's design are not present in this design. Thus the thermal analysis was based on a modified design that excludes final casing, see Figure 1.4. The benefits of a solid waste form and an irretrievable design are both monetary and political, as they reduce the cost of deep boreholes for minor actinide waste and the risk of sabotage.

4.3 Temperature Limits

The design of the deep geological waste canister suggested in this thesis is based on an evaluation of temperature and mass loading limits. Because of the relatively recent interest in exploring deep geological waste forms no regulations were found bearing on direct limitations

36

on the canister specified in this design. However there are many limitations of the materials and waste form that can be considered.

As mentioned in section 2, synroc and borosilicate glass can vitrify waste up to roughly thirty percent of their mass. Because a waste form loaded to thirty percent in either glass or synroc in the reference canister would produce peak temperatures far above the melting point of steel, mass loading will not be a limitation in this waste form design, even with the proposed annular design. However, the maximum temperature that each immobilization form can withstand, does limit the mass loading in each canister. For borosilicate glass, the literature review conducted for this thesis resulted in sources that reported varying maximum temperature limits. Volume twelve of the Scientific Basis for Nuclear Waste Management states that, "if the decision is made that the crystallization of borosilicate waste glasses must not occur within 10^6 years, a temperature of $200°$ C should not be exceeded" [28]. Yet, one study performed by researchers at the University of Sheffield states that the borosilicate glass transition temperature is $505°$ C [29]. In contrast, synroc is processed at temperatures between $1200°$ C and $1300°$ C [30]. At these temperatures other material limits must be taken into consideration, such as the melting point of the steel canister ($1300°$ C), and the melting point of granite [31].

Because there are no clear regulatory thermal limits on deep geological boreholes, the limits for the Yucca Mountain project are considered. One study notes that the maximum high level vitrified waste is $500°$ C, the maximum canister temperature is $375°$ C, and the maximum rock temperature can be between $250°$ C and $350°$ C [32]. Yet another study notes the maximum fuel pin temperature for transporting waste is $380°$ C [33]. It is this limit that provides the design basis for our analysis. It is important to note that this may not be an accurate reflection of future regulatory limits. Other suggested designs are also proposed for various maximum temperatures.

4.4 Immobilization Form (Glass or Synroc)

Given the above discussion concerning the maximum temperatures in borosilicate glass and synroc, synroc is the more appropriate waste form. Although there is clearly more industry

37

experience with borosilicate glass, synroc provides more assurance of meeting the design basis temperature. Borosilicate glass has been tested under many conditions. At temperatures greater than 250˚ C, it rapidly corrodes and devitrifies [34]. Not only can synroc withstand higher temperatures, but its thermal conductivity (2.1 W/mK) is nearly double that of borosilicate glass (1.1 W/mK) [35].

4.5 Minor Actinide Vitrified Waste Design

4.5.1 Annular Radius and Mass Loading

The reference linear heat rates calculated in chapter 2 yielded extremely high centerline temperatures for both glass and synroc waste forms which were on the order of thousands of degrees. In order to reduce the linear heat rate, and thus the centerline temperature, two features of the cylindrical waste form were altered: one geometric, and the other material. The two features are weight percent of minor actinides and annular radius. A decrease in the weight percent of minor actinides in the waste form will decrease its linear heat rate. Similarly, an increase in annular radius will decrease the linear heat rate. A linear heat rate of 552.5 W/m allows the synroc centerline temperature to be within the suggested design limitation for centerline temperature (380˚ C). A 552.5 W/m linear heat rate can be achieved with a minor actinide mass loading of 1% by weight and an annular radius of 8.5 cm.

Table 4.1 shows the maximum centerline temperatures in degrees Celsius as a function of various annular radii and minor actinide waste loading. As mentioned before, the maximum centerline temperature was conservatively based on the reference case of PWR assemblies with 60,000 MWD/MTIHM, ten years cooling, and a maximum granite temperature of 160˚ C. The dashed boxes in the table represent temperatures greater than the melting point of steel. The design parameters chosen (8.5 cm annular radius and 1% mass loading) result in a centerline temperature of 349˚ C. Economic analysis must be performed to assess the benefits of changing these parameters.

Table 4-1 Maximum Centerline Temperature in degrees Celsius of Synroc Waste form as a function of Minor Actinide Mass Loading and Annular Radius

Annular Radius (cm)

	2.5	4.5	6.5	8.5	10.5	12.5
0.1%	189.3	191	186.9	181	177	171
1.0%	471.78	426.76	388.1	349	306	258
2.0%	757.9	667.9	592.3	518	437	347
5.0%	-	-	-	1277	806	591
10.0%	-	-	-	-	-	988

(Row labels under "Mass Loading")

4.5.2 Design Specifications

The design specification for the designed waste form is shown in Table 4-2. These specifications reflect the 380° C temperature limit. It should be noted that the canister surface temperature and host rock temperatures are below regulatory temperatures for Yucca Mountain, 375° C and 350° C respectively. An alternate design, shown in Table 4-3, conveys the effect of increased maximum linear heat transfer rates on canister surface temperature and maximum granite temperature.

Table 4-2 Design Specifications of Minor Actinide Waste Form

Immobilization Form	Synroc
Annular Radius	8.5 cm
wt% Minor Actinide	1%
Max Linear Heat Transfer Rate	553 W/m
Max Centerline Temperature	349 C
Canister Surface Temperature	313 C
Granite Temperature	288 C

Table 4-3 Alternate Specifications of Minor Actinide Waste Form (With Increased Centerline Temperature)

Immobilization Form	Synroc
Annular Radius	9.0 cm

wt% Minor Actinide	2%
Heat Transfer Rate	1050 W/m
Centerline Temperature	498 C
Canister Surface Temperature	431 C
Granite Temperature	404 C

4.5.3 Convection, Conduction, and Radiation Heat Transfer Coefficients

It is important to note that radiation is the primary mode of heat transfer in the canister/wall gap. For the modified waste canister design specified in this chapter the comparative heat transfer coefficients are shown in Table 4.4. The proportionally large effective heat transfer coefficient for radiation compared to conduction and convection makes canister and granite surface emissivity key parameters in future designs.

Table 4-4 Heat Transfer Coefficients (W/m^{2}K) in Canister/Borehole Gap

	Conduction	Convection	Radiation
Design (Table 4-2)	0.79	0.91	19.60
Alternate Design (Table 4-3)	0.79	0.70	34.23

4.6 Technetium and Iodine Annular Plug

Although minor actinide waste presents most of the most challenging design problems in nuclear waste disposal, it is not the only group of radionuclides that severely impede long term storage design. Both technetium and iodine fission products produce many of the same design problems in nuclear waste management as minor actinides; Tc-99 and I-129 in particular, because of their long half lives and easy solublization, hence transportability. One modification to the design of the minor actinide waste form specified in section 4.5 is to fill the annular cylinder with vitrified technetium and iodine fission products. Table 4-5 shows the thermal power (in watts) of all technetium and iodine fission products from the reference case conditions as generated by ORIGEN. Table 4-6 shows the mass (in grams) of all technetium and iodine fission products.

40

Table 4-5 Thermal Power (Watts) of Technetium and Iodine Fission Products Generated by ORIGEN for Reference Conditions

	Time (years)					
	10	100	1000	10000	100000	1000000
Total Tc	0.011	0.011	0.011	0.011	0.008	0.000
Total I	0.000	0.000	0.000	0.000	0.000	0.000
Total	0.011	0.011	0.011	0.011	0.008	0.000

Table 4-6 Mass (Grams) of Technetium and Iodine Fission Products Generated by ORIGEN for Reference Conditions

	Time (years)					
	10	100	1000	10000	100000	1000000
Total	1716	1716	1712	1674	1347	437

The centerline temperature of a waste form consisting of an annular plug with thirty percent mass loading of technetium and iodine fission products is less than a degree hotter than its outer periphery. However, the thermal power of most of the iodine fission products decay away rapidly during the first ten years of cooling. Therefore, it must be noted that these calculations do not apply to waste that has not been cooled for ten years.

4.7 Tensile and Compressive Stress on Canister

According to Hoag's thesis the total mass of the waste string in the reference case design is less than 405MT [Hoag]. In his reference case, the packing material and assemblies have a mass of 516MT, bringing the total mass of the four kilometer waste string to 921MT. In this design, the PWR assemblies and packing materials are replaced with solid cylindrical waste forms that are five meters in length and have a diameter equal to that of the inner diameter of the canister. The mass of one five meter synroc waste form, including the technetium/iodine plug, is 1.70 MT. A two kilometer waste string in this case would make the total mass of the synroc waste form 680MT. Therefore the total mass of the minor actinide waste design (1085MT) is greater than that of the reference case in Hoag's thesis. This waste string must be subdivided into two or more sections and emplaced separately. The mass of one five meter synroc waste form, without the technetium/iodine plug, is 482MT, resulting in a total waste

string mass of 887MT. For continuity and mass production of canisters, the steel in this canister design should remain the same as that suggested by Hoag (T95 or C95).

It should be noted that the mass of synroc required to dispose of all technetium and iodine products in 100,000MT is roughly equivalent to the mass of three annular plugs.

4.8 Summary

The canister design proposed in this chapter is highly sensitive to allowable peak temperatures. Because of the lack of regulatory temperatures for deep geological boreholes, temperature limits for Yucca Mountain were considered as the design basis for the canisters. Given a maximum allowable centerline temperature of 380C, a synroc waste form was designed having an annular radius of 8.5 cm and loaded with 1% mass of minor actinide waste. The peak centerline temperature resulting from this design is 349C. The peak centerline temperature is not significantly changed by filling the annulus with maximum weight percent loaded synroc of technetium and iodine waste products because of their low thermal power after ten years cooling. However, the weight of the waste form with the technetium/iodine plug was greater than that of the reference case design. Therefore, the emplacement process should entail emplacing the waste in multiple stages. Synroc was used because it is better capable of handling the maximum allowable temperature and has greater thermal conductivity than borosilicate glass. The design need not be retrievable given the useless nature of minor actinide waste.

5 Economic Analysis

5.1 Introduction

The economic analysis in this chapter is a brief first order consideration of the major borehole-specific costs associated with deep geological minor actinide borehole disposal. The main comparison in the chapter is between minor actinide deep geological disposal, and intact spent fuel deep geological disposal.

5.2 Waste in Each Borehole

The mass of minor actinide waste contained in each annular waste form is 12.05 kg for the reference design specified in Table 4-2. Because 2.32 kg of minor actinide waste is generated from one initial metric ton of heavy metal, each canister contains roughly the minor actinide waste generated from 5.2MT initial of heavy metal. Each borehole is designed to accommodate 400 canisters, or the minor actinide waste generated from 2078MT of initial heavy metal. To accommodate the minor actinide waste in 100,000MT of spent PWR fuel, forty-nine boreholes would have to be drilled.

5.3 Cost Comparison to Total Spent Fuel

Using Hoag's estimate of a 10 million dollar borehole drilling cost, the estimated cost of drilling forty-nine boreholes is 490 million dollars [36]. This estimate represents 3.5% of the current 14 billion dollar nuclear waste fund. Hoag's estimated $50/kg of initial heavy metal for drilling boreholes for spent fuel is five times larger than the $9.6/kg initial heavy metal for drilling boreholes for just the minor actinide waste in the same amount of spent fuel. This

43

represents only 2.4% of the $400/kg initial heavy metal generated by the nuclear waste fund, based on a 1mill/kw-hr fee. Thus borehole-specific costs are essentially negligible.

5.4 Total Costs

The total costs of disposing of minor actinide waste by means of separation, waste form production, canister fabrication, and deep geological borehole emplacement are more than just the combined costs of drilling holes. In particular, the separation process may prove costly. However, in comparison to the alternative means of disposal once minor actinides are separated, namely repetitive transmutation, the costs of separation of minor actinides for deep geological disposal are singular. As noted in chapter 1, transmutation may require as many as seven separations before final annihilation of minor actinide wastes. Nevertheless separation and fabrication costs must be considered in further economic analysis of the viability of this approach. One must also consider the costs of licensing a borehole field for this application.

5.5 Summary

Deep geological boreholes for minor actinide disposal can be drilled for a fraction of the cost of drilling deep geological boreholes for intact spent fuel. Future economic analysis must be performed to assess the costs of separation and the other process steps involved. However, given the particularly limiting nature of minor actinide waste and the small fraction of the nuclear waste fund that it would take to drill deep geological boreholes for this waste, this option may be an attractive option to consider in conjunction with Yucca Mountain as an alternative to deep borehole disposal of spent fuel.

6 Summary, Conclusions, and Recommendations

The deep geological borehole concept for high level waste disposal has gained considerable interest in the past few years. However, research on the subject is still miniscule compared to that which has been performed on the reference United States Yucca Mountain Project. The viability of very deep boreholes as either a substitute-for or a complement-to the Yucca Mountain Project deserves serious consideration, especially for special applications such as minor actinide disposal. Since granite rock is present in all continents, this approach should be attractive on a global scale.

6.1 Thesis Summary

The largest advantage of separating minor actinide waste from spent nuclear fuel is the relative reduction in the stringency of constraints on nuclear fuel disposal. For such a small amount of PWR waste (less than 0.3% by weight), minor actinides account for many of the long-lived radionuclides in spent fuel. The elimination and subsequent disposal of minor actinides relaxes the challenges of estimating conditions in shallower mined geological facilities out to one million years. The energy calculations chapter of this thesis specifically identified the nature of minor actinide waste. Using results from ORIGEN each nuclide (listed in Appendix A-1) was evaluated on the basis of half-life, thermal power, and mass. This evaluation yielded three nuclides that dominate minor actinide thermal power (Cm-244, Am-241, and Am2-43). Thermal power given off by these nuclides account for nearly all of the decay heat of minor actinide waste from PWR's, for the reference case.

A reference linear heat rate was generated by evaluating the decay energies of the most significant radionuclides. Using this reference linear heat rate, a subsequent thermal analysis resulted in an annular waste form design that reduced the maximum linear heat rate to tolerable

45

limits. This effectively decreased thermal loading to meet the maximum centerline temperature limits for Yucca Mountain storage and transportation. A first order economic analysis of this design compared the costs of drilling boreholes for minor actinide waste, to that for intact spent fuel. It was also shown that technetium and iodine waste forms can be loaded within the annular hole, with virtually no affect on thermal performance. At only 20% of the capital costs of drilling boreholes for spent fuel, use of this approach for minor actinide (and technetium plus iodine) wastes could prove to be an advantageous strategy to complement the Yucca Mountain Project and that of similar shallow mined repository structures.

6.2 Future Work

6.2.1 Reference Borehole Concept

Further research is needed in many areas in support of this concept. Hoag's thesis mentions major areas such as site selection, borehole sealing, and chemical durability. Because this thesis heavily references Hoag's, the future work in terms of thermal analysis and stress calculations are similar.

6.2.2 Addition of Plutonium, Cesium, and Strontium

In addition to technetium and iodine (briefly analyzed in the evaluation), one area that is specific to extensions of this thesis is separation and deep borehole disposal of other very limiting nuclear waste products. Plutonium, cesium, and strontium carry significantly high heat loads. Plutonium nuclides, in addition, have very long half lives. It is likely that plutonium will not be separated from minor actinide waste in the near future, resulting in an inventory of so-called transuranic (TRU) wastes. Hence use of deep boreholes for TRU disposal is worth evaluation. Although plutonium and/or TRU recycle in LWR's is technically feasible, it would only extend uranium energy resources by 25% or so, which is not particularly attractive economically.

6.2.3 Economic Viability

The most important area in which future work must be performed is economic viability. To this end, a detailed analysis of the preliminary processes that take place prior to (and during) deep borehole emplacement is an essential part of assessing the viability of the overall project.

Appendix A: Table of Actinides

Table A-0-1 Commercial Waste Breakdown Results from ORIGEN for 60,000 MWD/MTHM Burnup, 10 year cooling, and Initial Mass of 1 MTIHM

	Heat (w)	Mass (gm)
Fission Products	1.71E+03 (68.62%)	6.12E+04 (6.12%)
Minor Actinide	5.60E+02 (22.46%)	2.60E+03 (0.26%)
Plutonium	2.23E+02 (8.92%)	1.47E+04 (1.47%)
Uranium	5.60E-02 (0.00%)	9.21E+05 (92.15%)
Total	2.50E+03 (100.00%)	1.00E+06 (100.00%)

Table A-0-2 PWR Waste date from ORIGEN for 60,000 MWD/MTHM Burnup, 10 year cooling, and Initial Mass of 1 MTIHM

Nuclide	Total Power after Ten Years (w/MTU)	Mass after Ten Years (g/MTU)	Comments
ac225	1.26E-08	6.20E-12	Negligible
ac227	1.27E-08	3.63E-07	Negligible
ac228	1.09E-12	6.27E-17	Negligible
am239	0.00E+00	0.00E+00	Negligible
am240	0.00E+00	0.00E+00	Negligible
am241	**9.47E+01**	**8.27E+02**	**Significant**
am242	2.17E-02	2.33E-05	Negligible
am242m	7.66E-03	1.81E+00	Negligible
am243	**2.63E+00**	**4.08E+02**	**Significant**
am244	0.00E+00	0.00E+00	Negligible
am244m	0.00E+00	0.00E+00	Negligible
am245	4.44E-12	3.76E-16	Negligible
am246	2.96E-14	1.85E-19	Negligible
at217	1.54E-08	2.24E-19	Negligible
bi208	0.00E+00	0.00E+00	Negligible
bi209	0.00E+00	2.28E-09	Negligible
bi210	1.67E-10	5.83E-13	Negligible
bi210m	0.00E+00	0.00E+00	Negligible
bi211	1.05E-06	6.31E-14	Negligible
bi212	1.24E-03	5.04E-09	Negligible
bi213	1.52E-09	1.86E-14	Negligible
bi214	5.00E-09	8.82E-15	Negligible
bk249	3.16E-08	9.87E-08	Negligible
bk250	5.85E-12	2.13E-16	Negligible
bk251	0.00E+00	3.52E-43	Negligible
cf249	4.71E-05	3.08E-04	Negligible
cf250	1.15E-04	2.82E-05	Negligible
cf251	1.99E-06	3.50E-05	Negligible
cf252	1.01E-04	2.61E-06	Negligible
cf253	0.00E+00	0.00E+00	Negligible
cf254	0.00E+00	5.30E-29	Negligible
cf255	0.00E+00	0.00E+00	Negligible
cm241	0.00E+00	0.00E+00	Negligible
cm242	5.70E-01	4.71E-03	Negligible
cm243	2.22E+00	1.17E+00	Negligible
cm244	**4.18E+02**	**1.48E+02**	**Significant**
cm245	**5.89E-02**	**1.03E+01**	**Negligible power, significant mass**
cm246	**2.61E-02**	**2.59E+00**	**Negligible power, significant mass**

49

Nuclide	Total Power after Ten Years (w/MTU)	Mass after Ten Years (g/MTU)	Comments
cm249	0.00E+00	0.00E+00	Negligible
cm250	1.06E-11	1.76E-10	Negligible
cm251	0.00E+00	0.00E+00	Negligible
es253	0.00E+00	0.00E+00	Negligible
es254	3.19E-11	4.44E-13	Negligible
es254m	0.00E+00	0.00E+00	Negligible
es255	0.00E+00	4.96E-40	Negligible
fr221	1.39E-08	2.07E-15	Negligible
fr223	8.87E-10	9.37E-15	Negligible
he4	0.00E+00	4.79E+00	Negligible
np235	5.28E-09	6.36E-08	Negligible
np236	7.61E-08	2.82E-03	Negligible
np236m	0.00E+00	0.00E+00	Negligible
np237	**1.84E-02**	**9.14E+02**	**Negligible power, significant mass**
np238	4.25E-04	3.29E-07	Negligible
np239	2.06E-01	3.51E-04	Negligible
np240	5.07E-17	4.17E-22	Negligible
np240m	2.46E-14	4.05E-20	Negligible
np241	0.00E+00	0.00E+00	Negligible
pa231	2.40E-06	1.67E-03	Negligible
pa232	0.00E+00	0.00E+00	Negligible
pa233	1.64E-03	3.10E-05	Negligible
pa234	5.84E-06	2.00E-10	Negligible
pa234m	1.51E-03	4.47E-10	Negligible
pa235	0.00E+00	0.00E+00	Negligible
pb206	0.00E+00	1.69E-10	Negligible
pb207	0.00E+00	7.29E-08	Negligible
pb208	0.00E+00	2.11E-04	Negligible
pb209	4.21E-10	7.80E-14	Negligible
pb210	1.70E-11	9.47E-10	Negligible
pb211	8.12E-08	1.07E-12	Negligible
pb212	1.40E-04	5.32E-08	Negligible
pb214	1.26E-09	1.19E-14	Negligible
po210	2.32E-09	1.61E-11	Negligible
po211	3.26E-09	6.98E-19	Negligible
po211m	0.00E+00	0.00E+00	Negligible
po212	2.51E-03	2.65E-19	Negligible
po213	1.78E-08	2.79E-23	Negligible
po214	1.81E-08	1.21E-21	Negligible
po215	1.17E-06	8.92E-19	Negligible
po216	3.03E-03	2.05E-13	Negligible
po218	1.41E-08	1.40E-15	Negligible
pu236	4.38E-03	2.41E-04	Excluded
pu237	3.46E-27	7.34E-28	Excluded
pu238	2.92E+02	5.14E+02	Excluded
pu239	1.19E+01	6.18E+03	Excluded

Nuclide	Total Power after Ten Years (w/MTU)	Mass after Ten Years (g/MTU)	Comments
pu242	1.48E-01	1.27E+03	Excluded
pu243	7.55E-09	2.52E-12	Excluded
pu244	1.28E-13	2.40E-07	Excluded
pu245	0.00E+00	0.00E+00	Excluded
pu246	5.50E-15	7.40E-17	Excluded
ra222	0.00E+00	0.00E+00	Negligible
ra223	9.35E-07	5.13E-10	Negligible
ra224	2.54E-03	4.64E-07	Negligible
ra225	2.61E-10	9.18E-12	Negligible
ra226	1.13E-08	3.94E-07	Negligible
ra228	7.79E-15	5.14E-13	Negligible
rn218	0.00E+00	0.00E+00	Negligible
rn219	1.09E-06	2.02E-15	Negligible
rn220	2.81E-03	8.01E-11	Negligible
rn222	2.13E-07	2.53E-12	Negligible
s250	0.00E+00	0.00E+00	Negligible
th226	1.00E+01	0.00E+00	Negligible
th227	9.47E-07	8.43E-10	Negligible
th228	2.42E-03	9.01E-05	Negligible
th229	1.11E-08	1.82E-06	Negligible
th230	3.53E-06	6.06E-03	Negligible
th231	1.10E-05	1.90E-08	Negligible
th232	6.53E-12	2.46E-03	Negligible
th233	0.00E+00	0.00E+00	Negligible
th234	1.27E-04	1.33E-05	Negligible
tl206	3.04E-16	4.39E-22	Negligible
tl207	7.73E-08	1.38E-13	Negligible
tl208	6.21E-04	8.97E-11	Negligible
tl209	1.26E-10	1.85E-17	Negligible
u230	0.00E+00	0.00E+00	Excluded
u231	0.00E+00	0.00E+00	Excluded
u232	2.55E-03	3.61E-03	Excluded
u233	1.58E-06	5.64E-03	Excluded
u234	3.43E-02	1.92E+02	Excluded
u235	2.80E-04	4.67E+03	Excluded
u236	1.06E-02	6.02E+03	Excluded
u237	5.79E-03	3.66E-05	Excluded
u238	7.77E-03	9.13E+05	Excluded
u239	0.00E+00	0.00E+00	Excluded
u240	3.93E-15	4.74E-18	Excluded
u241	0.00E+00	0.00E+00	Excluded

Table A-3 Mass and Thermal Power of Am-241 and Pu-241 as calculated by ORIGEN for Reference Scenario

Time (years)	Am-241 Power (watts)	Pu-241 Power (watts)	Am-241 Mass (grams)	Pu-241 Mass (grams)
10	94.71	3.969	827	1210
30	175.8	1.51	1536	459.5
100	203.9	5.14E-02	1781	15.63
300	149.4	5.83E-05	1305	1.77E-02
1000	48.68	5.20E-05	425.2	1.58E-02
3000	2.02	4.42E-05	17.65	1.34E-02
10000	2.62E-02	2.50E-05	2.29E-01	7.59E-03
30000	5.13E-03	4.88E-06	4.48E-02	1.49E-03
100000	1.70E-05	1.62E-08	1.48E-04	4.92E-06
300000	1.47E-12	1.33E-15	1.29E-11	4.05E-13
1000000	0.00E+00	0.00E+00	0	0

Appendix B: Calculations

Calculations for Mass of Am-241:

$$N_{initialAm-241} = 827g(\frac{6.022\times10^{23}\ nuclides/mol}{241.057\ g/mol}) = 2.07\times10^{24}\ atoms_{Am-241}$$

$$N_{initialPu-241} = 1210g(\frac{6.022\times10^{23}\ nuclides/mol}{241.057\ g/mol}) = 3.02\times10^{24}\ atoms_{Pu-241}$$

$$C = 2.07\times10^{24}\ atoms - \frac{0.048y^{-1}\cdot3.02\times10^{-24}\ atoms}{0.002y^{-1}-0.048y^{-1}} = 5.22\times10^{24}\ atoms$$

$$N_{Am-241}(t) = \frac{0.048\cdot3.02\times10^{24}}{0.002-0.048}e^{-0.048t} + 5.22\times10^{24}e^{-0.002t}$$

$$N_{Am-241}(t) = -3.15\times10^{24}e^{-0.048t} + 5.22\times10^{24}e^{-0.002t}atoms$$

$$Mass_{Am-241}(t) = [-1260.92e^{-0.048t} + 2089.53e^{-0.002t}]grams$$

Decay 1 Power versus Time calculations:

$$N_{Am-241}(t) = -3.15 \times 10^{24} e^{-0.048t} + 5.22 \times 10^{24} e^{-0.002t} \, atoms$$

$$P_{Am-241} = 5.6384 \text{MeV}(\frac{10^6 eV}{1\text{MeV}})(\frac{1.602 \times 10^{-19} watt - \sec}{1eV})(\frac{1day}{86400 \sec})(\frac{1year}{365 days})$$

$$(0.002 y^{-1})(-3.15 \times 10^{24} e^{-0.048t} + 5.22 \times 10^{24} e^{-0.002t})$$

$$P_{Am-241}(t) = 5.7285 \times 10^{23}(-3.15 \times 10^{24} e^{-0.048t} + 5.22 \times 10^{24} e^{-0.002t})$$

$$P_{Am-241}(t) = -180.45 e^{-0.048} + 299.03 e^{-0.002t} \, watts$$

Decay 2 Power versus Time Calculations:

$$N_{Cm-244}(t) = 3.652 \times 10^{23} e^{-0.038t} \, atoms$$

$$P_{Cm-244}(t) = 2.26 \times 10^9 \frac{J}{gm} \cdot 0.038 y^{-1} \cdot \frac{y}{365d} \cdot \frac{d}{86400s}$$

$$\cdot 3.652 \times 10^{23} e^{-0.038t} \, atoms \cdot \frac{mole}{6.022 \times 10^{23}} \cdot \frac{244.0627463 gm}{mole}$$

$$P_{Cm-244}(t) = 403.07 e^{-0.038t} \, watts$$

$$N_{Pu-240}(t) = 3.662 \times 10^{23}(-e^{-0.038t} + e^{-1.056 \times 10^{-4}t}) \, atoms$$

$$P_{Pu-240}(t) = 2.11 \times 10^9 \frac{J}{gm} \cdot 1.056 \times 10^{-4} y^{-1} \cdot \frac{y}{365d} \cdot \frac{d}{86400s}$$

$$\cdot 3.662 \times 10^{23}(-e^{-0.038t} + e^{-1.056 \times 10^{-4}t}) \, atoms \cdot \frac{mole}{6.022 \times 10^{23} atoms} \cdot \frac{240.0538075 gm}{mole}$$

$$P_{Pu-240}(t) = 1.0314(-e^{-0.038t} + e^{-1.056 \times 10^{-4}t}) \, watts$$

Power versus Time for decay 3:

$$N_{Am-243}(t) = 1.011 \times 10^{24} e^{-9.405 \times 10^{-5} t} atoms$$

$$P_{Am-243}(t) = 2.45 \times 10^{9} \frac{J}{gm} \cdot 9.405 \times 10^{-5} y^{-1} \cdot \frac{y}{365d} \cdot \frac{d}{86400s}$$

$$\cdot 1.011 \times 10^{24} e^{-9.405 \times 10^{-5} t} atoms \cdot \frac{mole}{6.022 \times 10^{23}} \cdot \frac{243.0613727 \text{gm}}{mole}$$

$$P_{Am-243}(t) = 2.9816 e^{-9.405 \times 10^{-5} t} watts$$

$$N_{Pu-239}(t) = 1.456 \times 10^{24} (-e^{-9.405 \times 10^{-5} t} + e^{-2.875 \times 10^{-5} t}) atoms$$

$$P_{Pu-240}(t) = 2.91 \times 10^{8} \frac{J}{gm} \cdot 2.875 \times 10^{-5} y^{-1} \cdot \frac{y}{365d} \cdot \frac{d}{86400s}$$

$$\cdot 1.456 \times 10^{24} (-e^{-9.405 \times 10^{-5} t} + e^{-2.875 \times 10^{-5} t}) atoms \cdot \frac{mole}{6.022 \times 10^{23} atoms} \cdot \frac{239.0521565 \text{gm}}{mole}$$

$$P_{Pu-240}(t) = 0.1533(-e^{-9.405 \times 10^{-5} t} + e^{-2.875 \times 10^{-5} t}) watts$$

Thermal Analysis

Important properties:

Thermal expansion coefficient of synroc: $\beta_{synroc} := 10.5 \cdot 10^{-6} \cdot K^{-1}$

Thermal conductivity of synroc: $k_{synroc} := 2.1 \dfrac{W}{m \cdot K}$

Thermal conductivity of steel: $k_{steel} := 50.2 \dfrac{W}{m \cdot K}$

Thermal conductivity of granite: $k_{granite} := 2.4 \cdot \dfrac{W}{m \cdot K}$

Thermal conductivity of air: $k_{air} := 0.036 \dfrac{W}{m \cdot K}$

Waste/Canister gap heat
transfer coefficient: $h_g := 31000 \dfrac{W}{m^2 \cdot K}$

Stephan- Boltzmann constant: $\sigma := 5.67 \cdot 10^{-12} \dfrac{W}{cm^2 \cdot K^4}$

Emissivity of steel (Schaum's Heat Transfer): $\varepsilon_1 := 0.8$

Emissivity of granite (from Internet search): $\varepsilon_2 := 0.45$

Density of synroc: $\rho_{synroc} := 4.35 \dfrac{gm}{cm^3}$

Limiting factors:

Maximum allowable centerline
temperature [36]: $T_{CLmax1} := 653K$

The earth's temperature gradient has been measured to be as high as 40 degrees Celsius per kilometer.
For an emplacement zone of 2km, corresponding to a total depth of 4km, the Earth's pre-emplacement
temperature could be as high as 160 degrees Celsius.

Earths Temperature Gradient: $T_{grad} := 160K$

Ambient Temperature of granite
at 4km depth: $T_{ambient} := 273.15K + T_{grad}$

Canister dimensions:

Outer diameter: $OD_{ws} := 339.7mm$ Outer radius: $r_{od} := \dfrac{OD_{ws}}{2}$ $r_{od} = 16.985\,cm$

56

Inner diameter: $\mathrm{ID}_{ws} := 315.32\,\mathrm{mm}$ Inner radius: $r_{id} := \dfrac{\mathrm{ID}_{ws}}{2}$ $r_{id} = 15.766\,\mathrm{cm}$

Waste/Canister gap thickness: $\delta_{gap} := \dfrac{\mathrm{ID}_{ws}}{2} \cdot \beta_{synroc} \cdot T_{CLmax1}$ $\delta_{gap} = 0.108\,\mathrm{cm}$

Waste-form radius: $r_o := \dfrac{\mathrm{ID}_{ws}}{2} - \delta_{gap}$ $r_o = 15.658\,\mathrm{cm}$

Bit sizes comonly used with the casing size used in this design have an outer diameter of 17.5 in, making the canister/borehole gap about 5 cm.

Canister/borehole gap: $\delta_{gap2} := \dfrac{17.5\mathrm{in} - \left(13 + \dfrac{3}{8}\right)\mathrm{in}}{2}$ $\delta_{gap2} = 5.239\,\mathrm{cm}$

Emplacement zone length: $L_{emp} := 2\mathrm{km}$

Canister length: $L_{canister} := 5\mathrm{m}$

Other Constants:

Semi-empirical correction factor [37]: $B := 7$

Universal Gas constant: $R_g := 8.3144\,\dfrac{J}{mol \cdot K}$

Atmospheric pressure: $P := 1\mathrm{atm}$

molecular weight of air: $m_{air} := 28.8\,\dfrac{gm}{mol}$

Linear heat rate

The mass of minor actinides in the glass as a function of weight percent is:

$$M_2(wt, R_1) := wt \cdot \left(\rho_{synroc} \cdot \pi \cdot L_{canister}\right) \cdot \left(r_{id}^2 - R_1^2\right)$$

$$q'_{eff}(R_1, wt) := 532\mathrm{W} \cdot \dfrac{1}{2.32\mathrm{kg}} \cdot \dfrac{M_2(wt, R_1)}{L_{canister}}$$

$$R_1 := 0.085 \cdot m$$

$$wt := 0.01$$

$$q'_{eff}(R_1, wt) = 552.531 \frac{W}{m}$$

Heat transfer from borehole wall to canister:

The heat transfer between the borehole wall and the canister's outer diameter is calculated below. First, the temperature of the borehole wall is calculated using a correlation relating the linear heat rate to borehole surface temperature. An effective thermal conductivity is then calculated by the summation of the conductivities due to conduction, convection, and radiation in air. The temperature of the outer canister wall is calculated using the effective thermal conductivity. An iterative process is then used to calculate the temperature of the outer canister wall.

Temperature at borehole wall:

The temperature of the borehole surface can be calculated from the maximum linear heat rate.

$$T_{granite} := T_{ambient} + \frac{q'_{eff}(R_1, wt)}{4 \cdot \pi \cdot k_{granite}} \cdot B$$

$$T_{granite} = 561.393 \text{ K}$$

Conduction and Convection

Let T_2 be the the temperature of the outer diameter of the canister wall.

$T_2 := 585.7K$ $\qquad$ $T_{granite} = 561.393 \text{ K}$ $\qquad$ $T_{avg} := \dfrac{T_2 + T_{granite}}{2}$ $\qquad$ $T_{avg} = 573.546 \text{ K}$

The quadratic equation for specific heat is an approximation based on data between 100 and 300 degrees Celsius. "L_{emp}" is the height of the emplacement zone, and delta is the distance between the two surfaces [38].

Density: $\qquad$ $\rho := \dfrac{P \cdot m_{air}}{R_g \cdot T_{avg}}$ $\qquad\qquad$ $\rho = 0.612 \dfrac{kg}{m^3}$

The dynamic viscosity is calculated using the Sutherland Equation for gases. The value calculated below is consistent with current data for air.[3]

$$\mu := \frac{1.464 \times 10^{-6} \cdot \left(\dfrac{T_{avg}}{K}\right)^{1.5}}{\dfrac{T_{avg}}{K} + 113.299} \cdot Pa \cdot s$$ $\qquad\qquad$ $\mu = 2.928 \times 10^{-5} Pa \cdot s$

Kinematic viscosity: $\qquad$ $v := \dfrac{\mu}{\rho}$ $\qquad\qquad\qquad\qquad$ $v = 4.784 \times 10^{-5} \dfrac{m^2}{s}$

Specific heat:
$$C_p := \left[0.0005 \cdot \left(\frac{T_{avg}}{K} - 273 \right)^2 + -0.3 \cdot \left(\frac{T_{avg}}{K} - 273 \right) + 1010 \right] \frac{J}{kg \cdot K}$$

$$C_p = 965 \frac{J}{kg \cdot K}$$

Grashof number:
$$Gr_b := \frac{g \cdot \left(T_2 - T_{granite} \right) \cdot \delta_{gap2}{}^3}{T_{avg} \cdot \nu^2}$$
$$Gr_b = 2.61 \times 10^4$$

Prandtl number:
$$Pr := \frac{C_p \cdot \nu \cdot \rho}{k_{air}}$$
$$Pr = 0.785$$

Rayleigh number:
$$Ra := Gr_b \cdot Pr$$
$$Ra = 2.049 \times 10^4$$

The correlation for conduction and convection within the gap is found in Fundamentals of Heat Transfer by M. Mikheyev. Keq1 is the effective thermal conductivity due to convection and conduction [38].

Correlation (Ra > 10^3):
$$k_{eq1} := k_{air} \cdot 0.18 \cdot Ra^{0.25}$$
$$k_{eq1} = 0.078 \frac{W}{m \cdot K}$$

Convection ratio:
$$\varepsilon_c := \frac{k_{eq1}}{k_{air}}$$
$$\varepsilon_c = 2.153$$

Accounting for the annular shape:

$$h_{eq1} := \frac{k_{eq1}}{\frac{OD_{ws}}{2} \cdot \ln\left(\frac{OD_{ws} + 2 \cdot \delta_{gap2}}{OD_{ws}} \right)}$$
$$h_{eq1} = 1.698 \frac{W}{m^2 \cdot K}$$

Radiation: The correlation for radiative heat transfer below was adapted from the Hoag's thesis [39]

$$h_{rad1} := \frac{\sigma}{\frac{1}{\varepsilon_1} + \left(\frac{OD_{ws}}{OD_{ws} + 2 \cdot \delta_{gap2}} \right) \cdot \left(\frac{1}{\varepsilon_2} - 1 \right)} \cdot \left(\frac{T_2{}^4 - T_{granite}{}^4}{T_2 - T_{granite}} \right)$$
$$h_{rad1} = 19.601 \frac{W}{m^2 \cdot K}$$

$$k_{rad1} := h_{rad1} \cdot \frac{OD_{ws}}{2} \cdot \ln\left(\frac{OD_{ws} + 2 \cdot \delta_{gap2}}{OD_{ws}} \right)$$
$$k_{rad1} = 0.895 \frac{W}{m \cdot K}$$

The canister outer wall temperature (T_2) is calculated below, and the iterative process was performed by updating T_2 until T_{2new} was within 0.01 degrees of T1.

$$k_{eff} := k_{rad1} + k_{eq1} \qquad T_{2new} := T_{granite} + q'_{eff}(R_1, wt) \cdot \frac{\ln\left(\frac{OD_{ws} + 2 \cdot \delta_{gap2}}{OD_{ws}}\right)}{2\pi \cdot k_{eff}}$$

$$T_2 = 585.7 \text{ K}$$

$$T_{2new} = 585.7 \text{ K}$$

The following numbers are provided for comparison:

$$h_{cond1} := \frac{k_{air}}{\frac{OD_{ws}}{2} \cdot \ln\left(\frac{OD_{ws} + 2 \cdot \delta_{gap2}}{OD_{ws}}\right)} \qquad h_{conv1} := h_{eq1} - h_{cond1}$$

$$h_{rad1} = 19.601 \frac{W}{m^2 \cdot K} \qquad h_{cond1} = 0.788 \frac{W}{m^2 \cdot K} \qquad h_{conv1} = 0.909 \frac{W}{m^2 \cdot K}$$

$$k_{eff} = 0.973 \frac{W}{m \cdot K}$$

Heat transfer from outer canister wall to centerline:

$$T_{CLmax2} := T_2 + q'_{eff}(R_1, wt) \cdot \left(\frac{1}{4 \cdot \pi k_{synroc}} + \frac{1}{2 \cdot \pi \cdot r_0 \cdot h_g} + \frac{1}{2 \cdot \pi \cdot k_{steel}} \cdot \ln\left(\frac{r_{od}}{r_{id}}\right)\right) - \frac{q'_{eff}(R_1, wt)}{4 \cdot \pi k_{synroc}} \cdot \left(1 - \frac{r_i}{r_{id}^2} \cdot\right.$$

$$T_{CLmax2} = 622.32 \text{ K}$$

Filling annulus with Tc and I:

The mass of all Tc and I fission products in the in the annulus as weight percent:

$$M_3(wt_1, R_1) := wt_1 \cdot (\rho_{synroc} \cdot \pi \cdot L_{canister}) \cdot (R_1^2)$$

$$q'_{annulus}(R_1, wt_1) := 0.0113 W \cdot \frac{1}{1.72 kg} \cdot \frac{M_3(wt_1, R_1)}{5m}$$

An annular inner radius of 8.5cm, and a 28% weight of Tc and I fission products will give a linear heat transfer rate within the annulus of 0.182 W/m and will not change the centerline temperature more than one thousandth of a degree. However, waste must cool for at least 10 years, otherwise the heat load for Tc and I will be significant.

$$wt_1 := 0.28$$

$$q'_{annulus}(R_1, wt_1) = 0.182 \frac{W}{m}$$

$$T_{CLmax3} := T_{2new} + \frac{q'_{annulus}(R_1, wt_1)}{4 \cdot \pi \cdot k_{synroc}} + q'_{eff}(R_1, wt) \cdot \left(\frac{1}{4 \cdot \pi k_{synroc}} + \frac{1}{2 \cdot \pi \cdot r_0 \cdot h_g} + \frac{1}{2 \cdot \pi \cdot k_{steel}} \cdot \ln\left(\frac{r_{od}}{r_{id}}\right)\right) - \frac{c}{}$$

$$\frac{q'_{eff}(R_1, wt)}{4 \cdot \pi \cdot k_{synroc}} = 20.938 \text{ K}$$

$$\frac{q'_{annulus}(R_1, wt)}{4 \cdot \pi \cdot k_{synroc}} = 2.458 \times 10^{-4} \text{ K}$$

$T_{CLmax3} = 622.328$ K

Economic Analysis:

Minor actinide waste:

$M_2(wt, R_1) = 12.048$ kg

Mass of Minor actinides from 1 MTHM, 10 years cooling:

$M_{ma} := 2.32$kg

$$\frac{M_2(wt, R_1)}{2.32 \text{kg}} = 5.193$$

$$M_{borehole} := \frac{M_2(wt, R_1)}{2.32 \text{kg}} \cdot 400 \qquad M_{borehole} = 2.077 \times 10^3$$

Tc and I waste:

$M_3(wt_1, R_1) = 138.231$ kg

$$\frac{M_3(wt_1, R_1)}{1.72 \text{kg}} = 80.367$$

Wasteform total mass:
With Tc and I centerfill:

$$M_{tot} := L_{canister} \cdot \pi \cdot \left(r_{id}^2 \right) \cdot \rho_{synroc}$$

$M_{tot} = 1.698$ tonne

Without Tc and I centerfill:

61

$$M_{tot2} := L_{canister} \cdot \pi \cdot \left(r_{id}^2 - R_1^2 \right) \cdot \rho_{synroc}$$

$$M_{tot2} = 1.205 \, tonne$$

References

1. Lester, R. K., Massachusetts Institute of Technology, Class 22.77: Nuclear Waste Management, Lecture 19: Economics and Finance, (2005).

2. Driscoll, M. J., "Boredom, the Weekly Newsletter on Deep Boreholes," vol. 1, no. 6, (Apr 2002).

3. McTaggart, Neil A., Gibb, Fergus G.F., Travis, Karl P., Burley, David., Hesketh, Kevin W. "Modelling Temperature Distribution Around Very Deep Borehole Disposals of HLW."

4. (2005, Dec.) Advanced Fuel Cycle Initiative. [Online]. Available: http://www.ne.doe.gov/infosheets/afci.pdf

5. "Global Nuclear Energy Partnership Launched." Nuclear Engineering International, vol. 51, no 620. (Mar 2006)

6. Visosky, Mark. "Actinide Destruction in a Thermal Spectrum Using Pressurized Water Reactors." MIT Thesis. (2005)

7. Bauer, Theodore H., Fanning, and Thomas H., Wigeland, Roald A. "Separations and Transmutation Criteria to Improve Utilization of a Geologic Repository." Nucl. Technol., vol. 154, p. 96 (2006)

8. Hoag, Ian C. "Canister Design for Deep Borehole Disposal of Nuclear Waste." MIT Thesis. (2005)

9. Fridman, E., Galperin, A., and Shwageraus, E. "Recycle of Transuranium Elements in Light Water Reactors for Reduction of Geological Storage Requirements." Nucl. Technol., vol. 153, (2006)

10. Ibid. p. 147

11. Ibid. p. 147

12. Ibid. p. 151

13. Ibid. p. 157

14. Visosky, Mark. "Actinide Destruction in a Thermal Spectrum Using Pressurized Water Reactors." MIT Thesis. (2006)

15. Gibb, F., and Chapman, N., "A Truly Final Waste Management Solution," Radwaste Solutions, (2003).

16. Hoag, Ian C. "Canister Design for Deep Borehole Disposal of Nuclear Waste." MIT Thesis. p. 39 (2006)

17. Ibid. p. 38

18. Croff, A.G., "ORIGEN2," Nucl. Technol., vol.62 (1983)

19. (2006, Feb.) Korea Atomic Energy Research Institute. [Online]. Available: http://atom.kaeri.re.kr/

20. Ibid.

21. (2006, Feb.) [Online]. Available: http://64.233.179.104/search?q=cache:eIDGhbRZJrsJ:www.eh.doe.gov/nepa/ea/ea0179/chap1.pdf+Borosilicate+glass+wt+%25+waste&hl=en&gl=us&ct=clnk&cd=2

22. (2006, Feb.) [Online]. Available: http://64.233.179.104/search?q=cache:eIDGhbRZJrsJ:www.eh.doe.gov/nepa/ea/ea0179/chap1.pdf+Borosilicate+glass+wt+%25+waste&hl=en&gl=us&ct=clnk&cd=2

23. Hoag, Ian C. "Canister Design for Deep Borehole Disposal of Nuclear Waste." MIT Thesis. (2006)

24. Ranade, Raj. "Thermal Simulation of a Deep-Borehole Storage Facility for Nuclear Waste." Research Science Institute. (Aug 2005)

25. Todreas, Neil E. and Kazimi, Mujid S., Nuclear Systems I, Thermal Hydraulic Fundamentals, Hemisphere Publishing Corporation, 1990, pg 13.

26. Mikheyev, M., Fundamentals of Heat Transfer, Peace Publishers, Moscow.

27. Hoag, Ian C. "Canister Design for Deep Borehole Disposal of Nuclear Waste." MIT Thesis. (2006)

28. Lutze, Werner. Ewing, Rodney C. "Scientific Basis for Nuclear Waste Management XII" Materials Research Society, Pennsylvania. p. 161, (1989)

29. Gibb, F., and Chapman, N., "A Truly Final Waste Management Solution," Radwaste Solutions, (2003).

30. (2006, Feb.) [Online]. Available: http://www.synrocansto.com/

31. (2006, May) [Online]. Available: http://education.jlab.org/qa/meltingpoint_01.html

32. Kuo, Wneg-Sheng., Driscoll, Michael, J., Tester, Jefferson W. "Reevaluation of the Deep-Drillhole Concept for Disposing of High-Level Nuclear Wastes." Nuclear Science Journal. Vol. 32, No. 3, (Jun. 1995).

33. Manteufel, R. D., and Todreas, N. E., "Effective Thermal Conductivity and Edge Conductance Model for a Spent-Fuel Assembly," Nuclear Technology, Vol. 105, (1994)

34. Lutze, Werner. Ewing, Rodney C. "Scientific Basis for Nuclear Waste Management XII" Materials Research Society, Pennsylvania (1989)

35. Lutze, Werner. Ewing, Rodney C. "Scientific Basis for Nuclear Waste Management XII" Materials Research Society, Pennsylvania (1989)

36. Manteufel, R. D., and Todreas, N. E., "Effective Thermal Conductivity and Edge Conductance Model for a Spent-Fuel Assembly," Nuclear Technology, Vol. 105, (1994)

37. Ranade, Raj. "Thermal Simulation of a Deep-Borehole Storage Facility for Nuclear Waste." Research Science Institute. (Aug 2005)

38. Mikheyev, M., Fundamentals of Heat Transfer, Peace Publishers, Moscow.

39. Hoag, Ian C. "Canister Design for Deep Borehole Disposal of Nuclear Waste." MIT Thesis. (2006)

40. Ibid.